

DEVELOPMENT OF 2D MoS₂ and Ni-DOPED MoS₂ MATERIALS AND THEIR APPLICATION

M.Sc. Thesis

By:
Rupak Das



DISCIPLINE OF PHYSICS
INDIAN INSTITUTE OF TECHNOLOGY INDORE
JUNE 2021

DEVELOPMENT OF 2D MoS₂ and Ni-DOPED MoS₂ MATERIALS AND THEIR APPLICATION

A THESIS

Submitted in partial fulfilment of the requirements for the award of the degree

of
Master of Science

By:
Rupak Das



DISCIPLINE OF PHYSICS
INDIAN INSTITUTE OF TECHNOLOGY INDORE
JUNE-2021



INDIAN INSTITUTE OF TECHNOLOGY INDORE

CANDIDATE'S DECLARATION

I hereby certify that the work which is being presented in the thesis entitled *Development of 2D MoS₂ and Ni-Doped MoS₂ Materials and Their Application* in the partial fulfilment of the requirements for the award of the degree of **MASTER OF SCIENCE** and submitted in the **DISCIPLINE OF PHYSICS, Indian Institute of Technology Indore**, is an authentic record of my own work carried out during the time period from July 2020 to June, 2021 under the supervision of Dr. Srimanta Pakhira, Assistant Professor.

The matter presented in this thesis has not been submitted by me for the award of any other degree of this or any other institute.

Rupak Das
12.06.21

Signature of the student with date
Rupak Das

This is to certify that the above statement made by the candidate is correct to the best of my/our knowledge.

Dr. Srimanta Pakhira
Assistant Professor and Ramanujan Faculty
Discipline of Physics
Indian Institute of Technology Indore
Khandwa Road, Simrol, Indore-453552, MP, India

17.06.2021
Signature of the Supervisor of

Dr. Srimanta Pakhira

Mr. Rupak Das has successfully given his/her M.Sc. Oral Examination held on **17th June, 2021**.

Dr. Srimanta Pakhira
Assistant Professor and Ramanujan Faculty
Discipline of Physics
Indian Institute of Technology Indore
Khandwa Road, Simrol, Indore-453552, MP, India

Signature(s) of Supervisor(s) of MSc thesis

Date: 17.06.2021

Sudip Chakraborty.

Signature of PSPC Member

Date: 18th June 2021

Signature of PSPC Member

Date: 18th June 2021

24-06-2021
Convener, DPGC

Date:

(DR. S. I. KUNDALWAL)

Signature of PSPC Member

Date: June 17, 2021

Contents

Abstract.....	10
Chapter 1	11
Introduction.....	11
1.1 What is a 2D material?	11
1.2 How do we make 2D materials?	11
Top-down.....	12
Bottom-up.....	14
1.3 Background:.....	15
1.4 General definitions:	18
1.5 Importance of 2-Dimensional Materials:	19
1.6 Application of Two-Dimensional Materials:.....	20
1.7 Motivation:.....	20
Chapter 2	22
Theoretical and Computational details.....	22
2.1 Density Functional Theory	22
2.1.1 DFT method:	22
2.1.2 Born-Oppenheimer Approximation.....	23
2.1.3 Hartree’s approximation.....	24
2.1.4 Hartree-Fock approximation.....	24
2.1.5 Ab initio method:	26
2.1.6 B3LYP method	27
2.1.7 Basis Sets:.....	28
<i>Type of Basis sets:</i>	29
2.1.8 Van der Waals (vdW) dispersion effects:	29
2.2 Computational Details:	31
2.2.1 For periodic system.....	31
2.2.1 For Non-Periodic system.....	32
Chapter 3	33
Hydrogen Evolution Reactions	33
3.1 What is HER?	33

3.2 What is electrolysis?	34
3.3 Water Splitting	35
3.4 How is hydrogen produced?	36
3.5 Hydrogen Fuel Cells	37
3.6 Electrocatalyst for hydrogen evolution reaction	38
Chapter 4	39
Results and Discussions	39
4.1 Results and Discussions	39
Conclusions:-	48
References	48

List of Figures

Figure 1: Each carbon atom in diamond (left) has bonds extending in 3 dimensions - meaning that when the diamond is cut in any orientation, some of these bonds must be broken and are left 'dangling' (shown in red).	12
Figure 2: Mechanical exfoliation involves peeling successive layers from a Van der Waals material using tape.	13
Figure 3: Liquid exfoliation often uses bubbles to force layers apart.	14
Figure 4: 2D materials MoS₂ & graphene	17
Figure 5: Transition metal dichalcogenides and Black phosphorus, layered metal Oxides and Hexagonal-boron nitride.	18
Figure 6: 2D MoS₂ and graphene	19
Figure 7: Application of 2D materials.	20
Figure 8: Density Functional Theory Method.	23
Figure 9: ab initio method.	27
Figure 10: B3LYP method.	28
Figure 11: Van der Waals dispersion effects of the atoms.	31
Figure 12: Hydrogen production in acidic medium.	34
Figure 13: Electrolysis of water.	35
Figure 14: Single atom Catalysts for Electrochemical Water Splitting.	36
Figure 15: Hydrogen production from steam reformation and Electrolysis.	37
Figure 16: Hydrogen fuel cells.	38
Figure 17: Electrocatalyst of the Ni based.	39
Figure 18: Band structure and density of states of the 2D monolayer pure MoS₂ material. (a) Top view and side view of the 2D 2H phase of the MoS₂ monolayer material, (b) band structure of the 2D MoS₂, and (c) total density of states calculations of the 2D monolayer.	41
Figure 19: Band structure and density of states Ni doped MoS₂ monolayer material. (a) Top view and side view of the 2D 2H phase of the Ni doped MoS₂ monolayer material, (b) band structure of the 2D Ni-MoS₂, and (c) total density of states calculations of the 2D.	42
Figure 20: Triangular shape crystal model	44
Figure 21: Hydrogen evolution reactions for the Ni doped MoS₂ material.	45

Figure 22: Hydrogen evolution reaction steps for the Ni-MoS₂ materials & optimized geometries of catalysts. 46

List of table

Table 1 : Lattice constants and angle, space group, average band length of the MoS₂ & Ni doped MoS₂ 41

Table 2 Energy calculations of the all the reactions mechanism steps Ni-MoS₂ materials in the gas phase. 47

ACKNOWLEDGEMENTS

*I would like to express my sincerest very special thanks and gratitude to my guide **Dr. SRIMANTA PAKHIRA**. It is an honor for me any times to work on a project under his guidance. It is my dignity to work on a research project at the **Department of Physics, IIT INDORE**. It was a good working experience in the excellent academic environment that the department and institute provided me with during the last two years. I express my earnest gratefulness to the institute and the department for providing such a good opportunity and provisions in providing me with such a great experience which will definitely help me in future while pursuing higher studies and my research. I would also like to express my happiness in being part a of the great research group. This group has taught me the didactics and strategy to be followed in research, how to find the destination of research and to use knowledge and skills within limited resources to produce significant contributions towards the progress of science. I would like to thank and express my sincerest gratitude to all the lab members including the research scientists, Ph.D. students, and my fellow **M.Sc.** students. And special thanks go to Ms. **Nilima Sinha** Mr. **Shrish Nath Upadhyay**, Mr. **Jena Akash Kumar Satrughna (Ph.D. scholar)** for their inseparable guidance, comprehensive help and for providing valuable information related to my understanding and performance of the work carried out.*

LIST OF PUBLICATIONS

Abstract

The two-dimensional layered sulphides (MoS_2 , VS_2 , WS_2) have activated acute scholarly interest. In this study, we are computationally and theoretically studied 2D monolayer MoS_2 and Ni doped MoS_2 materials. We found that the band structure and total density of states (DOS) using Crystal 17 and Crystal 14 suit codes from these materials. After we have studied Ni doped MoS_2 materials for the hydrogen evolution reaction (HER), which exhibits improved catalytic activity and good stability and neutral electrolytes for HER in gas medium with small overpotential. Density Functional Theory (DFT) study has been performing to clinch this research. The DFT calculation exhibits that the H_2 produce via Volmer-Heyrovsky mechanism from the reaction of the 2D monolayer Ni- MoS_2 material. All the reaction mechanisms were performed by Gaussian16 for both the MoS_2 and Ni- MoS_2 materials. 2D monolayer MoS_2 shows hydrogen Evolution Reaction (HER), and the activity and catalytic performance can be improved by Ni doping. Using DFT calculations, we found that this enhanced hydrogen evolution in the Ni- MoS_2 is predominantly because the lower energy barrier is built by a favourable overlap of the s-orbital of H_2 and d-orbital from the Ni transition metals with the lowest barrier energy occur for the Ni- MoS_2 materials.

Chapter 1

Introduction

1.1 What is a 2D material?

In materials physics, the term single-layer materials or 2D materials refers to crystalline solids consisting of a single layer of atoms. These materials are promising for some applications but remain the focus of research. Single-layer materials derived from single elements generally carry the “-ene” suffix in their names, e.g. graphene, Mexene, etc. Single-layer materials that are compounds of two or more elements have -ane or -ide suffixes. 2D materials can generally be categorized as either 2D allotropes of various elements or as compounds (consisting of two or more covalently bonding elements). Graphene was the first 'modern' 2D material to be isolated in 2004. Since then, there have been literally hundreds of other examples, with an extensive range of properties.

1.2 How do we make 2D materials?

It is possible to take any material and thin it down (until it has a thickness of only a few atoms) to create a 2D material. However, many materials (e.g. diamonds) have chemical bonds oriented in 3-dimensions, so thinning the material requires cutting these bonds – leaving them ‘dangling’. A 2D material created in this way will have a high density of dangling bonds, which are chemically and energetically unstable, and can force the material to rearrange its structure to lower its surface energy.

Another allotrope of carbon, graphite, has strong chemical bonds only along planes within the bulk material. These planes are stacked on top of each other and held together by weak van der Waals (vdW) interaction and so can be separated without leaving any dangling bonds. In the case

of graphite, a single plane is called graphene. Most of the 2D materials being studied therefore belong to the broader class of layered materials (or van der Waals materials).

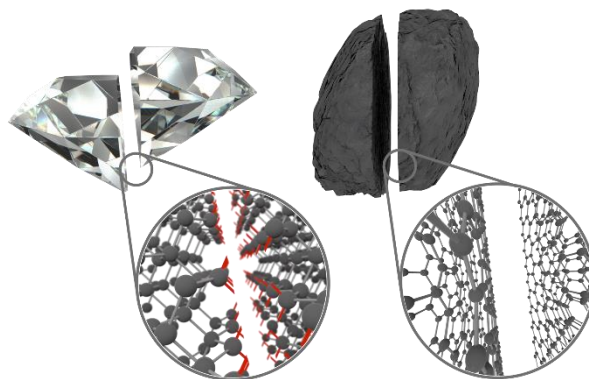


Figure 1: Each carbon atom in diamond (left) has bonds extending in 3 dimensions - meaning that when the diamond is cut in any orientation, some of these bonds must be broken and are left 'dangling' (shown in red).

There are two methods for making 2D materials:

- i) **Top-down** (starts with bulk material and makes it thinner)
- ii) **Bottom-up** (starts with the atomic ingredients and assembles them together)

Within each of these approaches are several subcategories, each with its own advantages and disadvantages - explained below.

Top-down

- **Mechanical exfoliation** – Commonly known as the ‘Scotch-tape method’, it was first used to create monolayer graphene. A piece of sticky tape is applied to the surface of layered material and then peeled off, taking flakes (consisting of a small number of layers) with it. The tape can then be pressed onto a substrate to transfer the flakes for study. The monolayer yield of this process is low (the flakes obtained are mostly multilayer), with no control over the size and shape. However, the size of monolayer flakes that can be produced is reasonable (from a few microns up to ~100 microns) and the quality of monolayers is excellent - with very few defects due to the lack of chemical processing involved.

It is also a suitable technique for all van der Waals materials. For these reasons, mechanical exfoliation remains popular for lab-based studies, but it is not scalable for integration into new technologies.

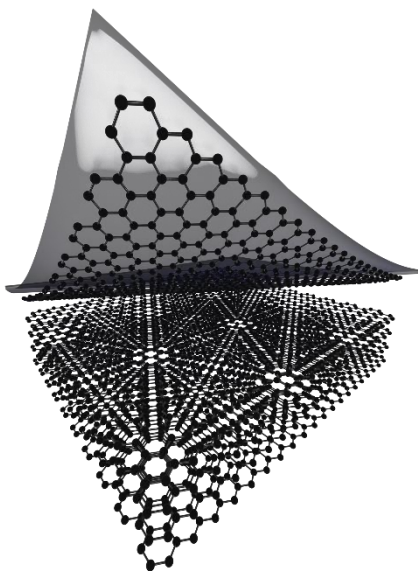


Figure 2: Mechanical exfoliation involves peeling successive layers from a Van der Waals material using tape.

Liquid exfoliation – Another mechanical method, liquid exfoliation, involves using an organic solvent as a medium to transfer mechanical force to the layered material (often in the form of a powder) suspended in the liquid. Sonication causes tensile stress to be applied to the layers, forcing them apart. To improve monolayer yield, variations exist, such as introducing reactive ions (between the material layers that create hydrogen bubbles) that push the layers apart or rapidly mixing the solution to create an additional shear force on the layers.

This method is highly scalable but has several drawbacks. The monolayer yield is again generally low, and the flakes are often less than 100 nm in size (due to the applied forces breaking them apart). The resultant flakes may also potentially have a high density of defects and residual solvent when removed from the solution, making them unsuitable for many optoelectronic applications.

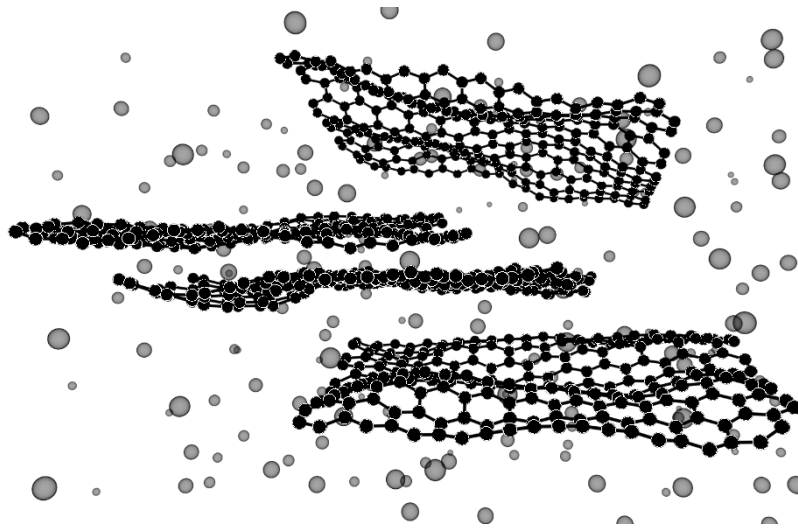


Figure 3: Liquid exfoliation often uses bubbles to force layers apart.

Bottom-up

- **Chemical vapor deposition** – This process involves passing one or more precursor gases (which usually contain the atomic ingredients of the required film) through a heated furnace, where they will react together or with a substrate and form a thin layer of the required material. This process has been successfully applied to grow graphene and TMDCs. Several parameters (such as gas pressures and compositions, temperature, and reaction times) need to be controlled as they will affect the thickness, quality and composition of the films. While this process is more complex and expensive than most top-down techniques, it is highly scalable, and the quality of the films produced approaches that of mechanically exfoliated layers.
- **Solution-based chemical synthesis** – A vast variety of techniques have been developed to synthesise 2D materials through wet chemical techniques. These include high-temperature chemical reactions in solution, interface-mediated growth (reactions occur only at the surface of a liquid), fusion of nanoparticles into larger nano sheets, and many more. Each method is particularly well-suited to a certain type of 2D material, and everything from graphene and TMDCs to monolayer metals can be synthesized using the appropriate technique.

The lateral size of the flakes produced by these methods is generally small (<100's nm), and the techniques share the same residual solvent problem as liquid exfoliation. However, for certain applications, the scalability, low cost and versatility of these techniques makes chemical synthesis the best method for large-scale production.

1.3 Background:

With the development of human society and the advancement of sciences technology, people have higher expectation for renewable energy source, which are mainly dependent on the efficiency of chemical reactions. According to statistics, more than 80% of chemical processes require catalysts to improve the corresponding reaction efficiency. Thus, catalysts play a vital role in the sustainable development of society with the growing interests on energy, with the rapid development of catalysts, the corresponding substrate is increasingly important for regulating the catalytic activity and stability of catalysts. Due to the unique 2D characteristic, 2D materials have been considered to be excellent substrates for supporting atomic catalysts and regulating their catalytic activity through the uniform and tractable compositional advantage of 2D materials. Thus, research on 2D materials is rising to an unprecedented height and will continue to remain a significant topic in the field of catalysts.

Research improvement of the advance materials for renewable energy applications has newly enticed important attention.¹⁻⁴ Hydrogen as a clean energy bearer has gained an attention in modern physics and renewable energy technology, and the hydrogen shows good promise as an alternative to fossil fuels because it is environmentally friendly. It has high energy density. In recent time, high pure hydrogen generated by water electrolysis is durable way compared to the traditional ways to produce low-purity hydrogen. In electrochemical water splitting, hydrogen evolution reaction (HER) acts as a remarkable technique.⁵ The good electrocatalysts are recognized Pt-group metals (PGM) hindered and their application comprehensive in hydrogen outturn, skilful and inexpensive earth enormous. For the acute inquiry, the HER catalysts are needed. Developing highly skilful and low cost catalysts on the part of the hydrogen evolution reaction (HER) still remains a great challenge in modern science and technology. Platinum is the most active and electrochemically stable catalyst for HER.⁶⁻¹⁰ Recently, two-dimensional (2D)

layered structure transition metal dichalcogenides¹¹ (TMDs) have been widely studied as a promising catalysts for HER, and among them monolayer molybdenum disulfide (MoS₂) has shown a great interest for the application of HER.¹²⁻¹⁵ Usually there are three type of strategies to enhance for the electrocatalytic capacity of MoS₂ catalysts (i) the number of manifested active sites are increasing (ii) the electrical contact to actuate site is ameliorative, and (iii) the intrinsic of every actuate site is enhancing. Following these strategies, for ameliorative the HER actuate of MoS₂ a great number of endeavor have been made¹⁶⁻²¹. We know that all the actuate sites of the MoS₂ are situated at the edges. HER undergo similar kinetic processes that reversibly bind hydrogen to the catalyst; therefore, the HER is restricted with it is slow kinetics for an important half- reaction of water splitting. Standard Hydrogen Electrode (SHE) requires a catalytic intermediate, which offers the potential to produce hydrogen. These reactions environ a catalytic intermediate. In recent times, earth plenty, 2D monolayer TMDs²² like MoS₂, WS₂ and W_xMo_{1-x}S₂ have obtained plenty attention as potential HER catalyst^{1,22,23}. So, in this work, we have performed a theoretical/computational study on the 2D monolayer MoS₂ and Ni-MoS₂ (noted as Ni-doped MoS₂) monolayer materials with their electronic properties for HER application. The electrolysis of water involves two reactions: Hydrogen Evolution Reaction (HER) and others is Oxygen Evolution Reaction (OER). During the HER process, in the electrolyte protons are absorbed and an over then waned into H₂ on the electrode when an over potential is applied. To curtail the overpotential, a catalyst is required to efficiently produce H₂. It has been found that the Pt is the most efficient electrocatalyst for HER because of its nearly zero overpotential in electrolytes²⁴⁻³². Recent experimental studies showed that the Ni doping plays a critical role in further enhancing the electrocatalytic HER performance of Ni-MoS₂ materials. This transition metal as a comprehensive, resourceful, and strong electrocatalytic activity electrode materials has been studied extensively and deeply, but Ni metal have a potent adsorption receptivity of hydrogen compared by the Nobel metal Pt. For HER the properties of Ni based materials are to be improved. Generally, there are two predominantly approaches for the improving its intrinsic activity and specific surface area is elaborate to improve the catalytic performance of Ni based materials one is alloying Ni and other is metal or non-metallic for example Ni-Mo^{33,34}, Ni-S³⁵. On the earth, the Hydrogen 10th best plenty components have been considered the ideal energy carrier in its molecular form H₂. The art of hydrogen manufacturing is called steam reforming from methane results in the emission of gaseous CO₂. In order to produce clean and renewable hydrogen

efficiently, the electrolysis of water becomes an ideal route since its discovery in 1789^{36,37}. To lower the catalysts cost, a natural abundant alternative and low-cost scalable synthesis are required. During the past years, naturally abundant MoS₂ coupled with other nanostructures started to gain more attention as HER catalyst³⁸⁻⁴⁰, after being ignored for their poor catalytic activity in the bulk form. However, due to the semiconducting character of MoS₂ and WS₂ (2H phase), poor electrical conductivity limits the HER kinetics. In order to take the advantages of the TMDs catalytic activity, conducting pathways are essential to accelerate the electron transport. Phase engineering, to convert the 2H phase into a metallic 1T phase, is an alternative to increase the intrinsic electrical conductivity due to a high electron density in the d orbitals of the metal⁴¹⁻⁴⁵. Besides phase engineering, the synthesis of heterostructures combining less-conducting TMDs with electrical conducting materials, such as graphene, MoS₂ materials seems to show significant promise⁴⁶. Two dimensional TMDs, graphene and others 2D materials etc. are shown in Figure 4 and 5 below

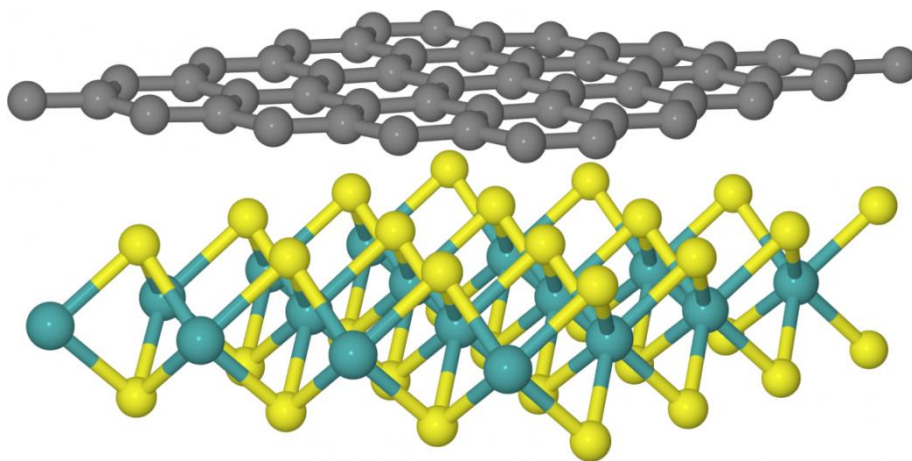


Figure 4:2D materials MoS₂ & graphene

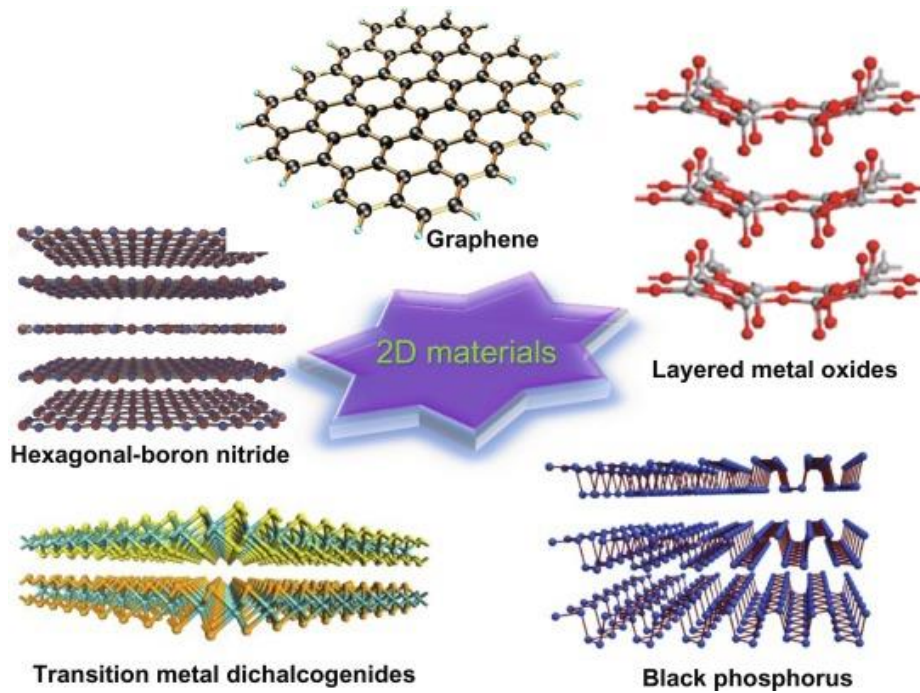
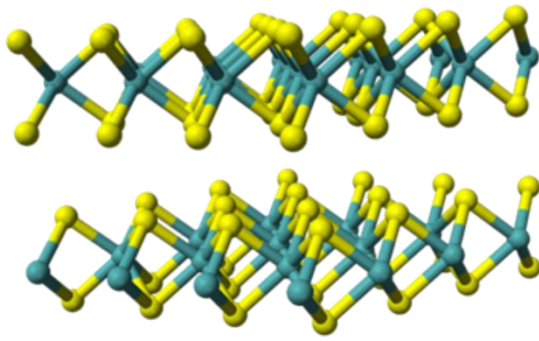


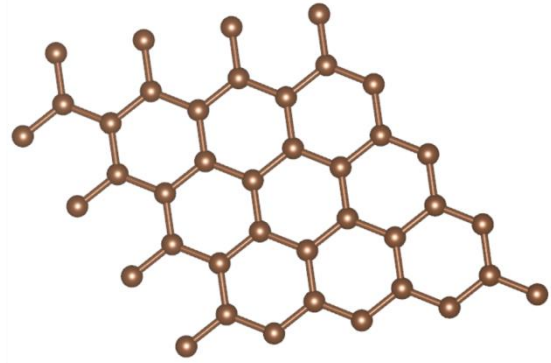
Figure 5: Transition metal dichalcogenides and Black phosphorus, layered metal Oxides and Hexagonal-boron nitride.

1.4 General definitions:

Two dimensional materials are defined as solid crystal consisting of a single or few layers of atoms having a typical thickness of 1-10 Å, and lateral dimension of tens of microns. It is below the Figure 6 for the MoS₂ and graphene (a) and (b)



(a)



(b)

Figure 6: 2D MoS₂ and graphene

1.5 Importance of 2-Dimensional Materials:

The 2-dimensional materials have distinct chemical and physical properties including layered structure, high surface area, layer-dependent optical band gap, and variation of chemical compositions. They have excellent properties and detection limits which are very important when sensitivity and measuring quanta are involved. The importance of 2D materials has been increased because of the problems in the miniaturization of modern electronic devices. At present, we have entered the era, where the modern laptops and smart phones are made with more than a billion transistors, but the conventional methods of further miniaturization of electronic devices for increased productivity are facing challenges. The key requirement in present time is to look beyond the silicon-based CMOS (Complementary Metal Oxide Semiconductor) technology and search for different alternatives, in which 2D crystals provide very interesting form-factors with respect to traditional 3D crystals. Although, devices made from 2D materials are still in the laboratory scale, but they have not failed to present strong promise for future. The high-mobility in these materials offers an alternative in the expanding field of low cost and large area electronics, which is currently dominated by low-mobility organic semiconductors and amorphous.

1.6 Application of Two-Dimensional Materials:

By exploiting the unique mechanical and electric transduction properties, 2D materials can be used in wide-ranging applications, including flexible electronics, strain sensors, optical sensors, nano generators, innovative nanoelectromechanical systems, etc. Two-dimensional (2D) inorganic materials at the quantum confinement limit are emerging as an important class of nanomaterials for novel applications in information technology, optoelectronics, spintronic, energy storage and conversion technologies^{47,48}. Recent advances in 2D materials started a new era of low-dimensional materials with extraordinary chemical and physical properties, ranging from insulators to semiconductors to metals and even superconductors. These materials are not only significantly different when compared to their bulk counterparts but also display unusual properties due to the much-enhanced quantum confinement in two dimensions and their high surface-to-volume ratios. 2D materials provide a wide range of structural, thermal, chemical, optical, magnetic, electrical, and mechanical properties that are otherwise unattainable. Application of 2-dimensional materials is given shown in Figure 7

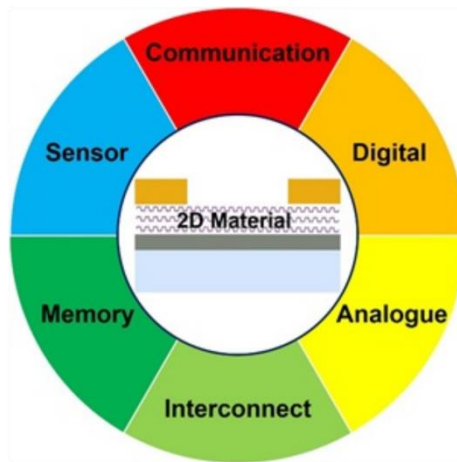


Figure 7: Application of 2D materials.

1.7 Motivation:

The increasing global demand for energy and the environmental consequences of burning fossil fuels have stimulated considerable effort to explore renewable carbon-free energy alternatives. Hydrogen is the cleanest fuel and represents one of the most promising energy

sources. The electrocatalytic HER is considered as one of the most important pathways to produce hydrogen efficiently. HER is one of the most important reactions in electrochemistry. Platinum is the most active and electrochemically stable catalyst. However, its high cost and low abundance have limited its utilization in the electrolysis of water. Thus, searching for alternative non-precious-metal electrocatalysts for the HER is a crucial task for hydrogen-based energy industry.

Chapter 2

Theoretical and Computational details

2.1 Density Functional Theory

2.1.1 DFT method:

Density Functionals Theory (DFT) is one of the most widely used quantum mechanical methods for calculations of the electronic structure (for ground state) of many body systems⁴⁹⁻⁵¹, in particular atoms, molecules, the condensed phases and surfaces, which achieve an excellent balance of accuracy and computational cost. However, for large molecules and atoms systems with few hundred atoms, the computational costs are very high. Therefore, there is a fast-growing demand for much more efficient implementation to utilize DFT for macro molecules. The basic idea behind this method is that the energy can be calculated for any electronic systems in terms of electron probability density. Density Functionals Theory (DFT) Applied on many electron systems from this systems we will found electron density of the system are given Figure:8 below. The theory behind all these things is named as DFT^{52,53}. We know how to solve the Schrodinger equation for the one-electron problem. But in the case of materials, we talk about the crystal. In a crystal, so many atoms present, and every atom has many electrons and many nuclei. This type of problem is called a many-body problem. For many-body problem, the solution of the time-independent, non-relativistic Schrodinger equation is given by

$$\hat{H} \Psi_i(\vec{x}_1, \vec{x}_2, \dots, \vec{x}_N, \vec{R}_1, \vec{R}_2, \dots, \vec{R}_M) = E_i \Psi_i(\vec{x}_1, \vec{x}_2, \dots, \vec{x}_N, \vec{R}_1, \vec{R}_2, \dots, \vec{R}_M)$$

Where H is the Hamiltonian for a system consisting of M nuclei and N electrons. Here x is the position of electron and R is the position of nuclei.

Where,

$$\hat{H} = -\sum_i \frac{\hbar^2}{2m_e} \nabla_i^2 - \sum_I \frac{\hbar^2}{2M_I} \nabla_I^2 + \frac{1}{2} \sum_{I \neq J} \frac{Z_I Z_J e^2}{|\vec{R}_I - \vec{R}_J|} - \sum_{i,I} \frac{Z_I e^2}{|\vec{r}_i - \vec{R}_I|} + \frac{1}{2} \sum_{i \neq j} \frac{e^2}{|\vec{r}_i - \vec{r}_j|}$$

Here, first two terms describe the kinetic energy of the electrons and nuclei. The other three terms represent the attractive electrostatic interaction between the nuclei and the electrons and repulsive potential due to the electron-electron and nucleus-nucleus interactions.

Dispersion-corrected Density functional theory (DFT-D)⁵⁴ abandons the many particle electron reality in favor of electron density. Constitutive relations constructed to relate energy to this density seek to capture the self-interactions of electrons.

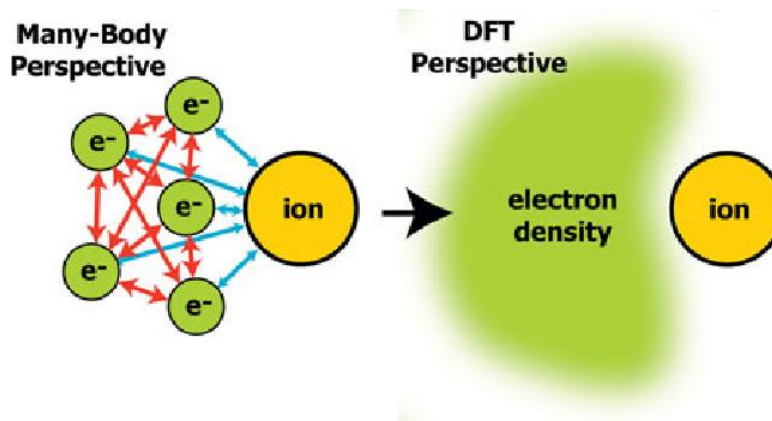


Figure 8: Density Functional Theory Method.

To solve this type of many-body problem Schrodinger equation, many approximations came. There is some approximation given.

2.1.2 Born-Oppenheimer Approximation

The Born-Oppenheimer Approximation is the assumption that the mass of the electron's negligible compares to the mass of nuclei. Due to their heavy masses compared to the electrons, the nuclei move much slower than the electrons. We can consider the electrons as moving in the

field of fixed nuclei. The nuclear kinetic energy is zero and their potential energy is merely a constant. Thus, the Hamiltonian reduces to

$$\hat{H} = -\sum_i \frac{\hbar^2}{2m_e} \nabla_i^2 - \sum_{i,I} \frac{Z_I e^2}{|\vec{r}_i - \vec{R}_I|} + \frac{1}{2} \sum_{i \neq j} \frac{e^2}{|\vec{r}_i - \vec{r}_j|}$$

Here the first term describes the kinetic energy of the electron, the second term describes attractive electrostatic interaction between the nuclei and electron and the third term describes repulsive potential due to electron-electron interaction.

2.1.3 Hartree's approximation

In this approximation, the multi-electron wave function can be expanded as a product of many single-electron wave functions. But we know electron wave function is anti-symmetric. But this approximation does not obey the Pauli Exclusion Principle. So here this approximation fails.

2.1.4 Hartree-Fock approximation

This approximation obeys the Pauli Exclusion Principle. In this approximation, the multi-electron wave function can be written as a Slater determinant.

Generalized Slater determinant wave function

$$\psi_{HF} = \frac{1}{\sqrt{N!}} \begin{vmatrix} \psi_1(\vec{x}_1) & \psi_2(\vec{x}_1) & \dots & \dots & \psi_N(\vec{x}_1) \\ \psi_1(\vec{x}_2) & \psi_2(\vec{x}_2) & \dots & \dots & \psi_N(\vec{x}_2) \\ \vdots & \vdots & & & \vdots \\ \psi_1(\vec{x}_N) & \psi_2(\vec{x}_N) & \dots & \dots & \psi_N(\vec{x}_N) \end{vmatrix}$$

The full expression of the Hartree-Fock equation is given by

$$\left[-\frac{\hbar^2}{2m_e} \nabla_i^2 + \hat{V}_{ext}(\vec{r}) + \sum_{j,\sigma_j} \int \psi_j^{\sigma_j*}(\vec{r}') \psi_j^{\sigma_j}(\vec{r}') \frac{e^2}{|\vec{r}-\vec{r}'|} d\vec{r}' \right] \psi_j^\sigma(\vec{r}) - \underbrace{\sum_j \int \psi_j^{\sigma_j*}(\vec{r}') \psi_j^{\sigma_j}(\vec{r}') \frac{e^2}{|\vec{r}-\vec{r}'|} \psi_j^\sigma(\vec{r}) d\vec{r}'}_{\text{Exchange term}} = \epsilon_i^\sigma \psi_i^\sigma(\vec{r})$$

Here the exchange term is only non-zero when considering electrons of the same spin. The effect of exchange on the many-body system is that electrons of like spin tend to avoid each other. As a result of this, each electron has a hole associated with it which is known as the exchange hole (or the Fermi hole). This is a small volume around the electron that like-spin electrons avoid. The charge contained in the exchange hole is positive and exactly equivalent to the absence of one-electron.

Hohenberg-Kohn Theorems

Theorem -1: The external potential is a unique functional of electron density.

Theorem -2: The ground state energy can be obtained variationally: the electron density that minimizes the total energy is the exact ground-state electron density.

Kohn-Sham Equation

Kohn-Sham equation is a Schrodinger like equation for non-interacting particles within the effective potential, where the wave function is electron density.

Schrodinger like equation

$$\left[-\sum_i \frac{\hbar^2}{2m_e} \nabla_i^2 + \left[\frac{\hat{V}_{ext}(\vec{r}) + \hat{V}_{cl}(\vec{r}) + \hat{V}_{xc}(\vec{r})}{\hat{V}_{eff}[\vec{r}]} \right] \right] \phi_i(\vec{r}) = \epsilon_i \phi_i(\vec{r})$$

Exchange Correlation Functional

To solve the Kohn-Sham equation we used some exchange-correlation functional approximation.

1: Local Density Approximation (LDA)

This approximation assumes that the density can be treated as a uniform electron gas; the exchange-correlation energy at each point in the system is the same as that of a uniform electron gas of the same density. This approximation holds for a slowly varying density. The exchange-correlation energy for a density is given by

$$E_{xc}^{LDA}[\rho(\vec{r})] = \int \rho(\vec{r}) \varepsilon_{xc}(\rho) d\vec{r}$$

Here the exchange-correlation energy is only depending on electron density. For inhomogeneous systems, this approximation fails.

2: Generalized Gradient Approximation (GGA)

As the LDA approximates the energy of the true density by the energy of local constant density, it fails in situations where the density undergoes rapid changes such as in molecules. An improvement to this can be made by considering the gradient of the electron density. The exchange-correlation energy

$$E_{xc}^{GGA}[\rho(\vec{r})] = \int \rho(\vec{r}) \varepsilon_{xc}[\rho, \nabla\rho] d\vec{r}$$

Here the exchange-correlation energy is depending on electron density and gradient of electron density.

2.1.5 Ab initio method:

Ab initio quantum chemistry methods are computational chemistry methods based on quantum chemistry. The ab initio means “from first principal” or from the beginning”, implying

that the only inputs into an ab initio calculation are physical constants. Ab initio quantum chemistry methods attempt to solve the electronic Schrodinger equation give the positions of the nuclei and the number of electrons in order to yield useful information such as electron densities, energies and other properties of system. These ab initio methods^{55,56} apply for metals that have nanometre dimensions that is electronic (quantum mechanics).

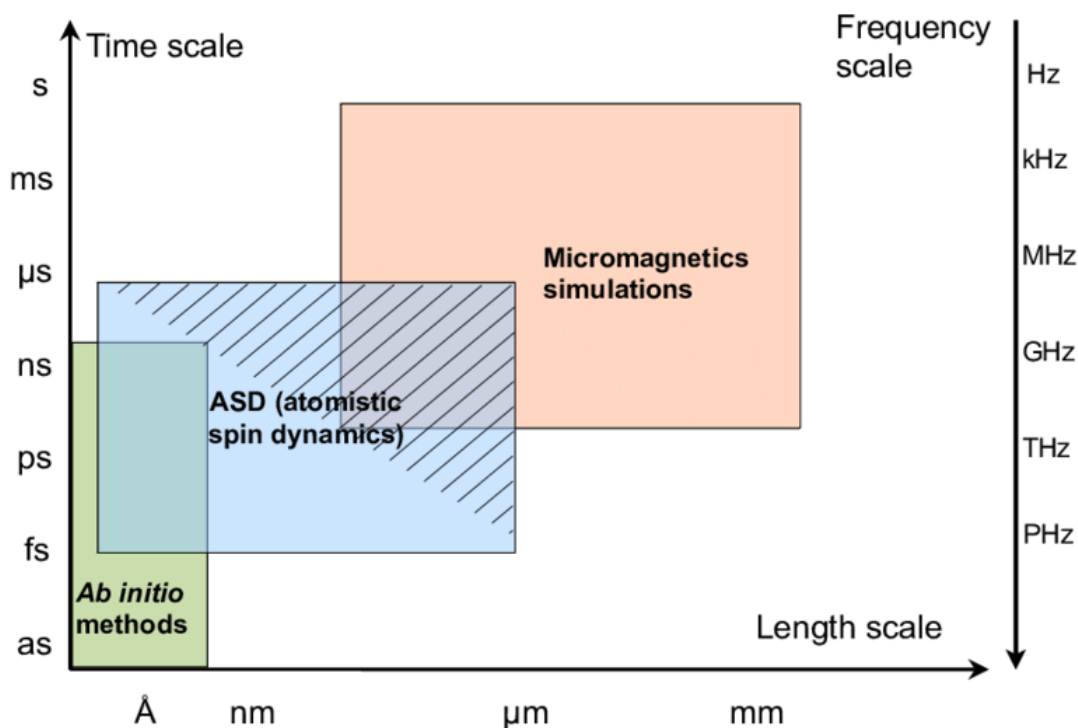


Figure 9: ab initio method.

2.1.6 B3LYP method

B3LYP is a hybrid functional developed in the late 1980s. It turns out that DFT and Hartree-Fock (HF) based methods are basically trying to do the same thing - recover electron correlation. However, they have different difficulties, Hartree-Fock methods exactly treat exchange correlation but have difficulties recovering dynamic electron correlation while DFT has

an exact form for dynamic electron correlation but since DFT is not quantum mechanical, it must approximate exchange correlation.

B3 is Becke's three parameter exchange correlation functional which uses three parameters to mix in the exact Hartree-Fock exchange correlation and LYP is the Lee Yang and Parr correlation functional that recovers dynamic electron correlation. B3LYP is popular for many reasons. It was one of the first DFT methods that was a significant improvement over Hartree-Fock. B3LYP is generally faster than most of the Post Hartree-Fock techniques and usually yields comparable results. It is also fairly robust for a DFT method. B3LYP is a functional, which includes exact exchange and GGA corrections in addition to LDA electron-electron and electron-nuclei energy. The weights of the parts were fit to reproduce geometry of a test suite of small molecules. As such use of B3LYP for calculations with heavier atoms is questionable.

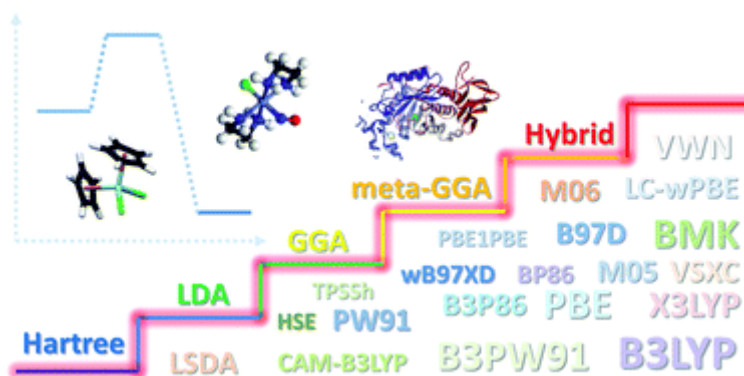


Figure 10: B3LYP method.

2.1.7 Basis Sets:

A basis set in theoretical and computational quantum physics and chemistry is a set of functions is called basis function. It is used to represent the electronic wave function in the Hartree-Fock and DFT methods.

Type of Basis sets:

- Minimal basis sets.
- Double zeta and triple zeta etc.
- Slater type orbitals basis set.
- Gaussian type orbitals basis sets.
- Split-valence basis sets.
- Diffuse basis sets.

2.1.8 Van der Waals (vdW) dispersion effects:

The study of intermolecular or non-covalent vdW interactions has long been key to our understanding of complex molecular systems, particularly when considering the assembly of molecules into supramolecular systems or condensed matter. Predicting and studying cohesion in molecular materials relies heavily on accurate and physically realistic treatments for the different intermolecular forces that arise in such materials, with those that result from instantaneous fluctuations of electrons, which are referred to as dispersion or van der Waals (vdW) interactions.^{57–60} Although, they are typically weaker than electrostatic interactions or hydrogen bonding, their long-ranged nature and ubiquity in all molecular systems means they can always play an important role in non-covalent bonding. Indeed, as they scale with system size, in some cases strongly non-linearly, their importance can grow for larger molecules and molecular assemblies.

Dispersion interactions⁶¹ are quantum-mechanical in nature and they used to form part of the correlation energy of a system. They stem from the inherent zero-point fluctuations of electrons on an atom, which give rise to instantaneous multipole moments. These moments induce multipole moments on other atoms, which then interact with the original moment. The leading order contribution is from dipole–dipole interactions, with a $1/R^6$ dependence on distance.

The ability of an atom to form such moments (both instantaneous and induced) depends on its polarizability. The polarizability of an atom is influenced by its chemical bonding but also by its environment through polarization and induction effects, where it is changed by coupling to the electric field of its surrounding atoms. Such effects are known to be non-additive in nature and

they are important for going beyond simple point charges in the modelling of electrostatics in force fields, and modelling molecular polarizabilities.

However, despite the central role of polarizability in vdW interactions³⁹, the vast majority of models ignore its non-additive and non-local nature, using simple pairwise-additive models with dispersion coefficients that do not capture any dependence on non-local environment. In neglecting many-body effects, these methods often require empirical fitting of parameters to a given molecule and environment.

Many of the developments in our understanding of vdW interactions in molecular systems have taken place in the context of vdW-inclusive DFT.⁵³ Workhorse semi-local and hybrid density functionals neglect long-range correlation and considerable progress has been made in augmenting semi-local density functionals with non-local vdW contributions. However, many of these vdW-inclusive DFT^{38,62} approaches are still founded on pairwise models of dispersion interactions, as use of fully *ab initio* approaches, such the random-phase approximation, is not feasible due to their far higher computational cost than standard semi-local DFT.

Despite their successful application in many areas, including occasional successes for crystal-structure prediction, quantitative and qualitative failures remain when employing pairwise models of vdW interactions. As a result, in recent years there has been considerable interest in studying and modelling non-additive and many-body contributions to vdW interactions, which can take a number of forms. In this perspective piece, we focus on collective effects in vdW interactions in molecular materials, with a particular emphasis on non-additivity in polarizabilities and techniques that can capture these effects, including the recently established many-body dispersion (MBD) approach. We demonstrate fresh insights into the significance of collective vdW effects on the stability and characteristics of molecular materials using a variety of applications. The reader is directed to recent works on a variety of various approaches to the problem for a more in-depth explanation of the theory and physics of many-body vdW interactions.

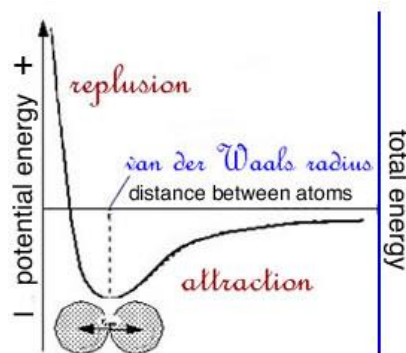


Figure 11: Van der Waals dispersion effects of the atoms.

2.2 Computational Details:

2.2.1 For periodic system

In this computational methodology, the hybrid periodic B3LYP-D3 DFT⁶³⁻⁶⁵ is taken account to obtain the equilibrium crystal structures including optimized unit cell geometries, materials and electronic properties⁶⁶ of our system material of interest. The periodic equilibrium structures and properties calculations of the designed material is being performed computationally with the application of *ab initio* method through CRYSTAL17 suite code^{67,68}. This CRYSTAL17 code is used for Gaussian type basis sets rather than plane wave function in order to obtain the better productive results that can coincide with the experimental data. In this computational method, it is necessary to account for the vdW dispersion effects for better understanding as there are many weak long- range vdW interactions between the atoms and the layers of the crystal⁶⁹⁻⁷². Taking account, the above interaction, Grimmes semi- empirical third order (-D₃) dispersion correction is included in the present DFT computations that takes care of all the long – range vdW interactions. When the system is covalently bonded in a layered manner and the layers are weakly bonded then in that case, vdW dominated by long range dispersion force then in that cases DFT-D functional theory can be employed to obtain a very accurate geometry and other thermochemical properties^{62,73-76}. For simplicity, B3LYP - D3 method have been found to be noted as DFT- D. To

specify the Gaussian type of atomic orbital of different atoms; Triple- zeta valence with polarization function quality (TZVP)⁷⁵ basis sets were used for the Sulphur (S) and Nickel (Ni) atoms while HAYWSC-311(d31) G type basis set with Hay-wadt type effective core potentials (ECPs) is used for Molybdenum (Mo) atoms in the crystal structure calculations for all the systems studied for this project. The convergence threshold has been set at 10^{-7} a.u. to evaluate the convergence of the energy, forces, and electron densities⁷⁷⁻⁸¹ For the crystal structure and electronic properties calculation, the spin contamination effects has been reduced in the present computation work as the DFT-D method (B3LYP-D3) provides an enhanced quality geometry^{63,65,71,82}. It was found that the density as well as energy are being less affected with the application of the above computational method^{83,84}.

Once the optimized structure for both of the MoS₂ and Ni-MoS₂ materials were obtained, electronic properties such as band structure and density of state (DOS) calculations were performed by taking into the application of B3LYP-D3 computational method. For the geometric optimization, a set of Monkhorst⁸⁵-pack k-point grids were carried out, and similarly a set of Monkhorst-pack k-mesh grids are used for the systems electronic properties calculations, i.e calculation of both of the band structure and density of states calculations. This k-point grids are in general used for the integrations of the first brillouin zone. The atomic orbitals of the Sulphur (S) and Molybdenum, Nickel (Ni) atoms were used to compute and plot the total density of states of the pristine MoS₂ and Ni- MoS₂ material systems, respectively. VESTA, is a visualization code, is used to reproduce the graphics and to analyze the crystal structures of all the systems studied here⁸⁵.

2.2.1 For Non-Periodic system

We adopted a cluster model system consisting of 9-Mo atoms, 21-S atoms with single Ni doped atom and is used to investigate Hydrogen Evolution Reaction (HER) mechanism computationally including reaction barrier energy of the Ni-MoS₂ material. This cluster model has inert basal plane and active edges; Ni doping makes it active at the planner surface by having extra valence electrons free to make bonds and to take in the reaction mechanism. Mo6L-DFT

method^{86,87} is used to study the HER mechanism of the prepared cluster system with the use of 6-31+G** basis sets for Hydrogen (H), Sulphur (S), and Nickel (Ni) atoms⁸⁸, and LANL2DZ basis sets with Effective Core Potentials (ECPs) for Molybdenum (Mo) atoms⁸⁹. The DFT-Mo6L method is found to provide the reliable energy barriers for the chemical reaction mechanism. After that we utilized the Polarizable continuum model for all of the calculations. In these calculations including optimization of the reactants and transition states to capture solvation consequence in the DFT. For the Heyrovsky reaction mechanism, we are used four water molecules were added explicitly. For the polarizable continuum model (PCM) calculations, dielectric constants (k) of the water are used 78.35. And all computations for the HER mechanisms were performed with the general-purpose electronic structure quantum chemistry program Gaussian16⁹⁰ to get the optimized geometries and transition structure for the model.

Chapter 3

Hydrogen Evolution Reactions

3.1 What is HER?

The hydrogen evolution reaction (HER) $2\text{H}^+ + 2\text{e}^- \rightarrow \text{H}_2$ is the cathodic reaction in electrochemical³⁴ water splitting. The HER is of a two-electron transfer reaction with one catalytic intermediate, and it offers the potential to produce H_2 , a critical chemical reagent and fuel. Driving the HER with renewable sources of hydrogen fuel that can stored, transported and used in a zero-emission fuel cell of combustion engine. Achieving high energetic efficient for water splitting requires the use of a catalyst to minimize the overpotential necessary to drive the HER. Platinum is the best-known catalyst for HER and requires very small over potentials even at high reaction rates in acidic solution.

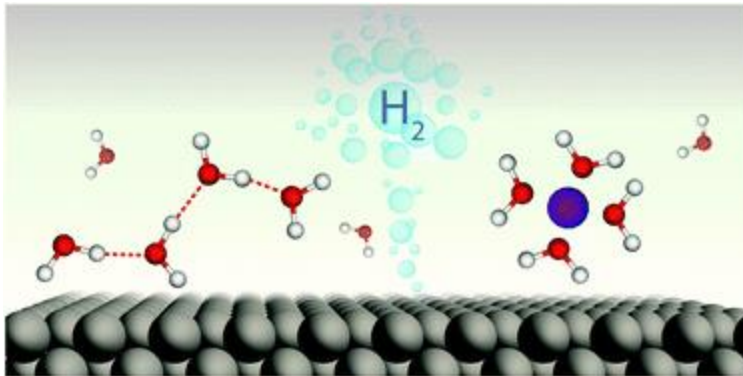


Figure 12: Hydrogen production in acidic medium.

3.2 What is electrolysis?

Electrolysis process by which electric current is passed through a substance to effect a chemical change. The chemical change is one in which the substance loses or gains an electron (oxidation or reduction). The process is carried out in an electrolytic cell, an apparatus consisting of positive and negative electrodes held apart and dipped into a solution containing positively and negatively charged ions. The substance to be transformed may form the electrode, may constitute the solution, or may be dissolved in the solution. Electric current enters through the negatively charged electrode (cathode); components of the solution travel to this electrode, combine with the electrons, and are transformed (reduced). The products can be neutral elements or new molecules. Components of the solution also travel to the other electrode (anode), give up their electrons, and are transformed (oxidized) to neutral elements or new molecules. If the substance to be transformed is the electrode, the reaction is often one in which the electrode dissolves by giving up electrons.

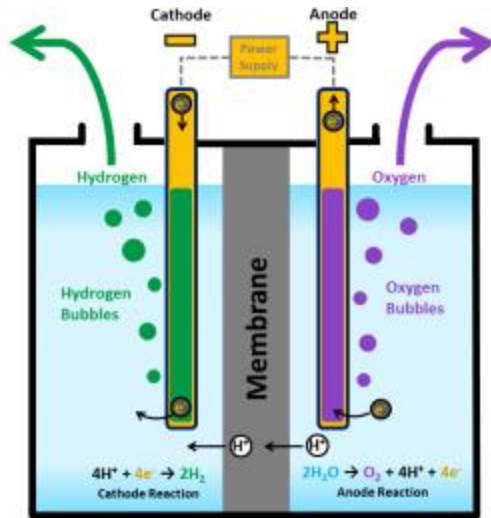
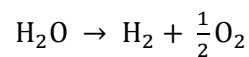


Figure 13: Electrolysis of water.

Electrolysis is used extensively in metallurgical processes, such as in extraction or purification of the metals from compounds and in deposition of metals from solution and hydrogen and oxygen are produced by the electrolysis of water.

3.3 Water Splitting

Electrochemical water splitting can be performed in a variety of devices, which can be broadly classified into two main categories: water electrolysis and water photolysis. Water electrolyzers, which include polymer electrolyte membrane (PEM), alkaline, and solid oxide electrolyte configurations, require energy input from an external source of electricity to drive the water splitting process. Photo electrochemical (PEC) and photo catalytic water splitting devices rely on semiconductor materials to absorb sunlight and generate excited charge carriers and can therefore split water without an external electricity input. Regardless of the device configuration, the overall water splitting reaction remains the same:

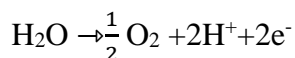


In a water splitting cell, the hydrogen evolution reaction (HER) takes place at the cathode and the oxygen evolution reaction (OER) takes place at the anode. These reactions are shown below, as they occur in acidic electrolyte:

Hydrogen evolution reaction (HER)



Oxygen evolution reaction (OER)



To split water efficiently, catalysts are required for both the HER and the OER.

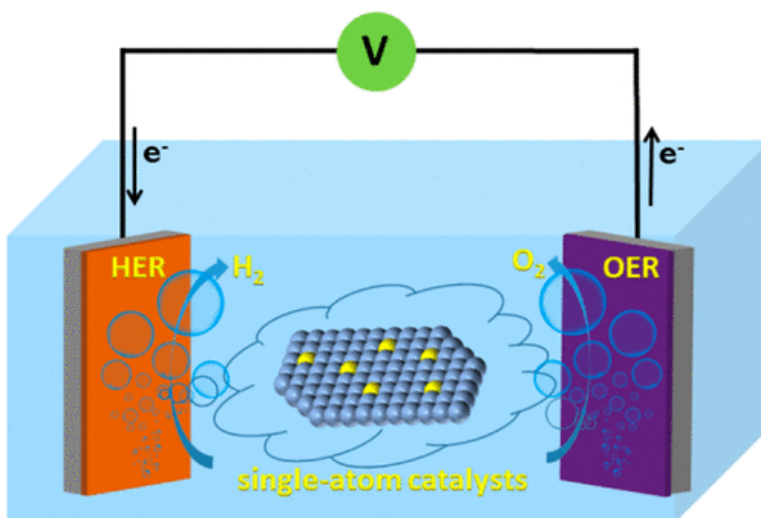


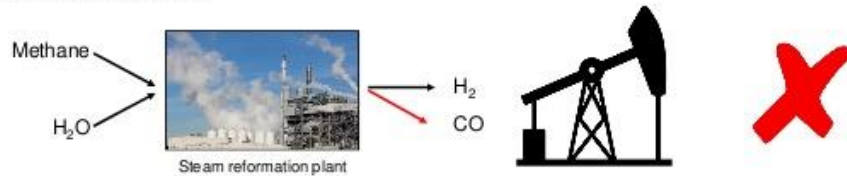
Figure 14: Single atom Catalysts for Electrochemical Water Splitting.

3.4 How is hydrogen produced?

To produce hydrogen, it must be separated from the other elements in the molecules where it occurs. There are many different sources of hydrogen⁸² and ways for producing it for use as a fuel. The two most common methods for producing hydrogen are steam-methane reforming and electrolysis (splitting water with electricity). Researchers are exploring other methods.

Hydrogen Production

- Steam reformation:



- Electrolysis:

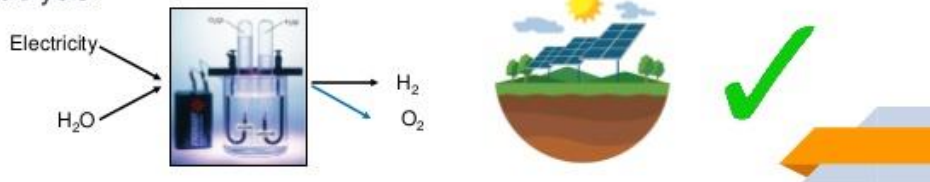


Figure 15: Hydrogen production from steam reformation and Electrolysis.

3.5 Hydrogen Fuel Cells

A fuel cell combines hydrogen and oxygen to produce electricity, heat, and water. Fuel cells are often compared to batteries. Both convert the energy produced by a chemical reaction into usable electric power. However, the fuel cell will produce electricity as long as fuel (hydrogen) is supplied, never losing its charge.

Fuel cells are a promising technology for use as a source of heat and electricity for buildings, and as an electrical power source for electric motors propelling vehicles. Fuel cells operate best on pure hydrogen. But fuels like natural gas, methanol, or even gasoline can be reformed to produce the hydrogen required for fuel cells. Some fuel cells even can be refilled directly with methanol, without using a reformer.

In the future, hydrogen could also join electricity as an important energy carrier. An energy carrier moves and delivers energy in a usable form to consumers. Renewable energy sources, like the sun and wind, can't produce energy all the time. But they could, for example, produce electric energy and hydrogen, which can be stored until it is needed. Hydrogen can also be transported (like electricity) to locations where it is needed.

Hydrogen Fuel Cells

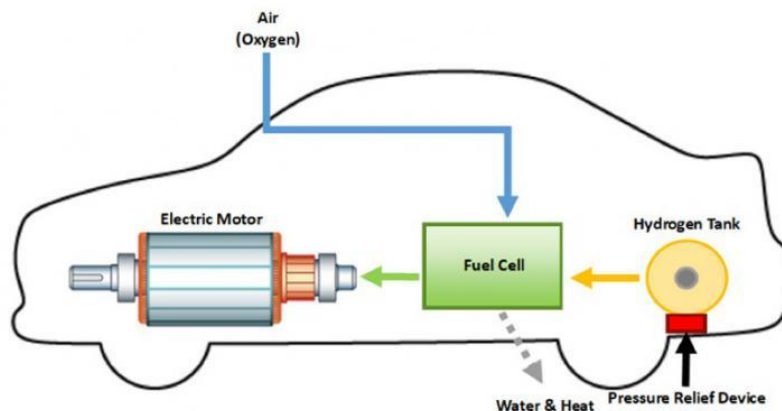


Figure 16: Hydrogen fuel cells.

3.6 Electrocatalyst for hydrogen evolution reaction

An electrocatalyst is a catalyst that participates in electrochemical reactions. Electrocatalysts are a specific form of catalysts that function at electrode surfaces or, most commonly, may be the electrode surface itself. An electrocatalyst⁹¹ can be heterogeneous such as a platinumized electrode. Homogeneous electrocatalysts, which are soluble, assist in transferring electrons between the electrode and reactants, and/or facilitate an intermediate chemical transformation described by an overall half-reaction. Major challenges in electrocatalysts focus on fuel cells.

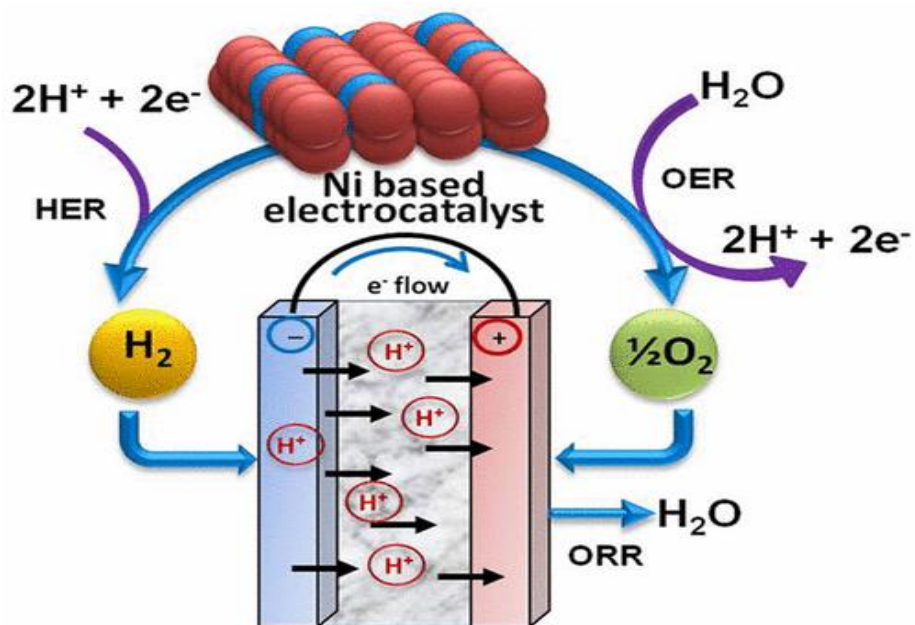


Figure 17: Electrocatalyst of the Ni based.

Chapter 4

Results and Discussions

4.1 Results and Discussions

The equilibrium structure⁴⁹, geometry, lattice parameters and electronic property calculations of the pristine 2D monolayer 2H phase of the MoS₂ material were obtained by the

B3LYP-D3 computational method. Visualization of the obtained optimized geometry of the 2D MoS₂ is presented in Figure 18 (a). Lattice constants of this pristine 2D single layer MoS₂ were found to $a = b = 3.176 \text{ \AA}$ and $\gamma = 120^\circ$ with P-6m2 symmetry, which was found to be in consistent with the previously reported literatures and is well harmonized with the experiment results.³ From the electronic property calculations of this material, it was observed that the 2D MoS₂ material has a direct bandgap at K point and the band gap energy is about 2.53 eV, which is shown in Figure 18(b) below and it agrees well with the experimental observation and earlier theoretical results.³ These findings signify that the pristine 2D MoS₂ may not be an useful electrocatalyst for the applications of HER processes due to its large band gap which makes it to give non conducting property and inert basal plane. It is also found that there is no electronic density around the Fermi level (E_F) in the total density of states calculations of the 2D MoS₂ as shown in the Figure 18(c).

The optimized geometry of the Ni doped MoS₂ material is represented in the Figure 19(a). It has been observed that the lattice constants for this Ni doped MoS₂ materials were found to have the values as, $a=b=9.511 \text{ \AA}$ and adjacent angle $\alpha=\beta=90^\circ$, $\gamma=120^\circ$ with P-6m2 symmetry. Further, from the electronic property calculations of this Ni-MoS₂ material it was observed that the Ni doped MoS₂ material has band gap value zero which is shown in Figure 19(b) which makes it a conductor. The transformation of MoS₂ from a high band gap semi-conductor to a conductor due to the Ni transition metal doping (providing free electrons at its d subshell free electrons) which results a large contribution towards the total density of states of Ni-MoS₂, as depicted in d subshell density of states plot in the figure 19(d). We have also observed that total density of states is large around the Fermi level, same can be visualized from the Figure 19(c) and the d subshell density of state of the Ni doped MoS₂ material clearly support the previous statement. Ni atom doping at the edge size of MoS₂ makes is possible for electron accumulates in conduction and valence band that enables electron mobility. As per electrochemistry, the crucial contribution of the electrocatalyst is to help in the reaction for transferring electrons between the electrode and reactants without being actively chemically reacted. So, from the above computational work it can be confirmed that the 2D Ni-doped MoS₂ might be very much helpful in enhancing the intermediate chemical transformation in HER process.

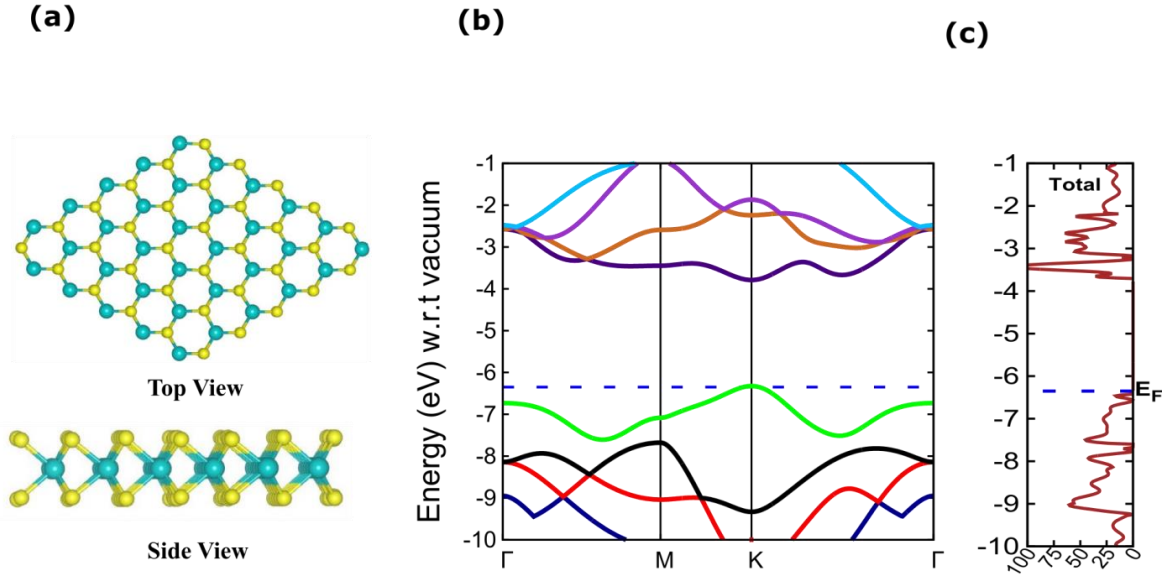


Figure 18: Band structure and density of states of the 2D monolayer pure MoS₂ material. (a) Top view and side view of the 2D 2H phase of the MoS₂ monolayer material, (b) band structure of the 2D MoS₂, and (c) total density of states calculations of the 2D monolayer.

Table 1 : Lattice constants and angle, space group, average band length of the MoS₂ & Ni doped MoS₂ optimize structure.

Materials	MoS ₂	Ni doped MoS ₂
Adjacent angle (α & β in degree)	90.0°	90.0°
Lattice Constants (a=b)	3.219	9.511Å
Angle (γ in angle)	120.0°	120.0°
Average bond distance.	Mo-S=2.39Å	Mo-S=2.411Å Ni-S=2.390Å
Space group symmetry.	P6m2	P1

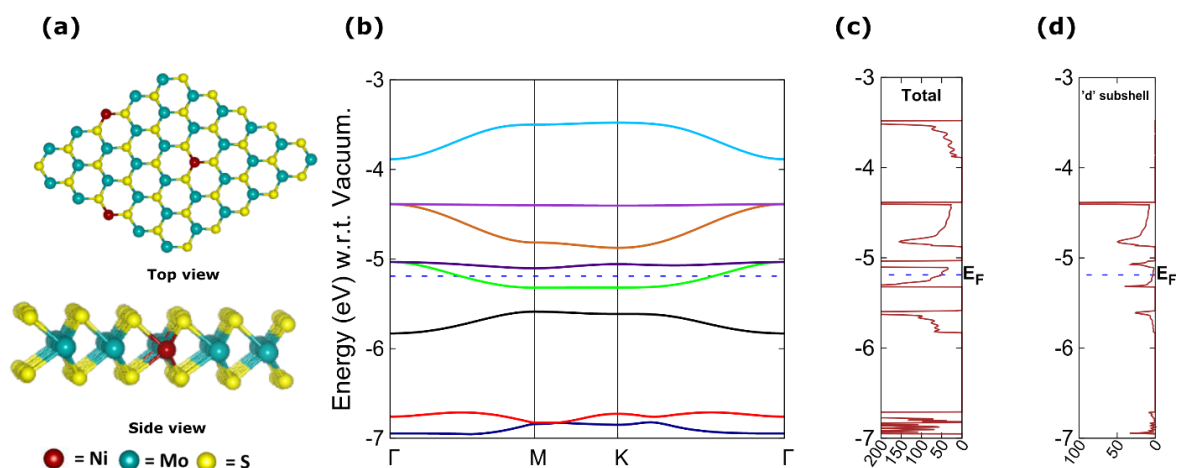
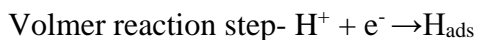


Figure 19: Band structure and density of states Ni doped MoS₂ monolayer material. (a) Top view and side view of the 2D 2H phase of the Ni doped MoS₂ monolayer material, (b) band structure of the 2D Ni-MoS₂, and (c) total density of states calculations of the 2D

In this study,⁹² we have chosen triangular shape crystal model for the HER as shown in below Figure 20. First of all our main target we develop new electrocatalyst materials for processes including hydrogen evolution reactions. This reaction is needed for H₂ production through electrolysis of water and generation electricity in Hydrogen fuel cells. We design new electrocatalyst Ni doped MoS₂ material with improved performance. We have doped 12.5% Ni within MoS₂ materials. In this approach, we have investigated the catalytic activity of the Ni-MoS₂ material for HER. We mentioned that the study of reaction barriers energy is necessary to explain the chemical reactivity of the catalyst, instead extrapolating the kinetic effects from the electronic ground state properties which explain only about equilibrium thermodynamics. We are deliberated two types of difference reactions footing with the most eminent. One is Volmer reactions steps and other one is Heyrovsky reaction steps. In case of Volmer reaction is Hydrogen (H) atom migrates from the Sulphur (S) atom to the transition metal Nickel (Ni) that is, H* migration is called as the Volmer reaction mechanism. And in case of Heyrovsky reaction is on a number of electrodes the second step in hydrogen evolution is the reaction of a proton with an adsorbed hydrogen intermediate to form a H₂ molecule, which is known as the Heyrovsky reaction

mechanism. As generally, HER mechanism can be describe to the following two possible footing in the acidic electrolyte.



Here H_{ads} is an adsorbed hydrogen atom on the catalyst surface, and Volmer –Heyrovsky reaction through H_2 can be produced. In the Volmer reaction mechanism the rate determining step is the migration of a hydrogen atom. But in case of Heyrovsky reaction mechanism the rate determining step requires an adjacent hydronium (H_3O^+). It is the source of a proton along the reaction pathway involving adsorbed H^- atoms form H_2 . It was found that these two reaction footing have the lowest barriers energy for Hydrogen Evolution Reaction (HER) of the Ni-MoS₂ materials. The energy barriers are shown in Table 2. These calculations are published only catalytic activity of the alloy Ni-MoS₂ materials, which agrees as well as with the experiment observation. Most interestingly, DFT calculations for the Ni-MoS₂ materials alloy has the highest reaction energy barriers for H_2 formation, when compared to solvent phase value. More specifically, the activation energy barrier in the gas phase for H_2 evolution following the Heyrovsky reaction mechanism of the Ni-MoS₂ materials alloys is 21.6 kcal/mol, and the experimental value(solvent phase) 1.478 kcal/mol for H_2 formation. From this results we can say The Ni-MoS₂ material shows an excellent catalytic performance in HER. And the one very importance reactions is H^* migration or Volmer reactions mechanism in the HER is still running.

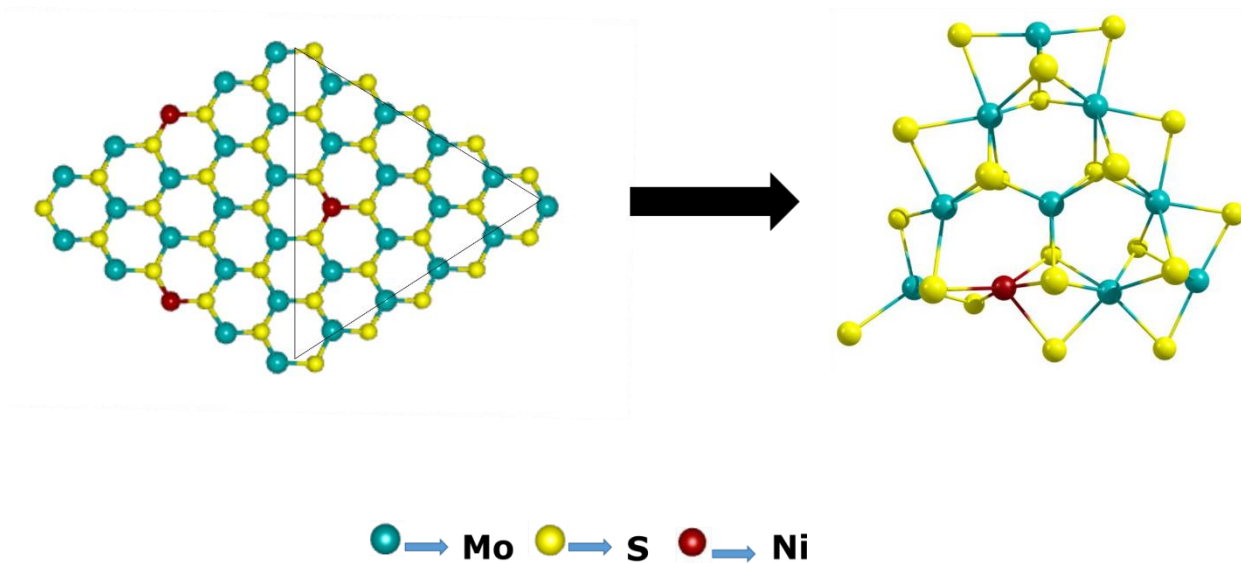


Figure 20: Triangular shape crystal model

For the H₂ evolution on the Ni-MoS₂ materials below the chemical reaction mechanism by using the Density functional Theory (DFT) method with the M06-L functional method. From This method we are found accurate Gibbs free energies for the all the reaction steps or all reaction barrier involving transition metal states (TMs). The H* migration reaction barrier is Volmer reaction mechanism. The Volmer reaction mechanism mark in the dotted red circle below figure and we are produced H₂ using Heyrovsky reaction mechanism, highlight in a dotted blue circle on the Ni-MoS₂ materials. The chemical reaction mechanism^{76,93} for the Ni-MoS₂ materials following the steps.

model system in the DFT calculations. The transition states are occurred in the H^* migration reaction of this material figure (e) and the position of the atoms Hydrogen atom (H) are between the Sulphur and Nickel. The Volmer transition states are mark by a red dotted circle (e). In case of Heyrovsky reaction transition states (TSs) are occurred this material above figure (h) and we can see clearly the position of the H_2 in the transition states is highlight by a dotted red circle.

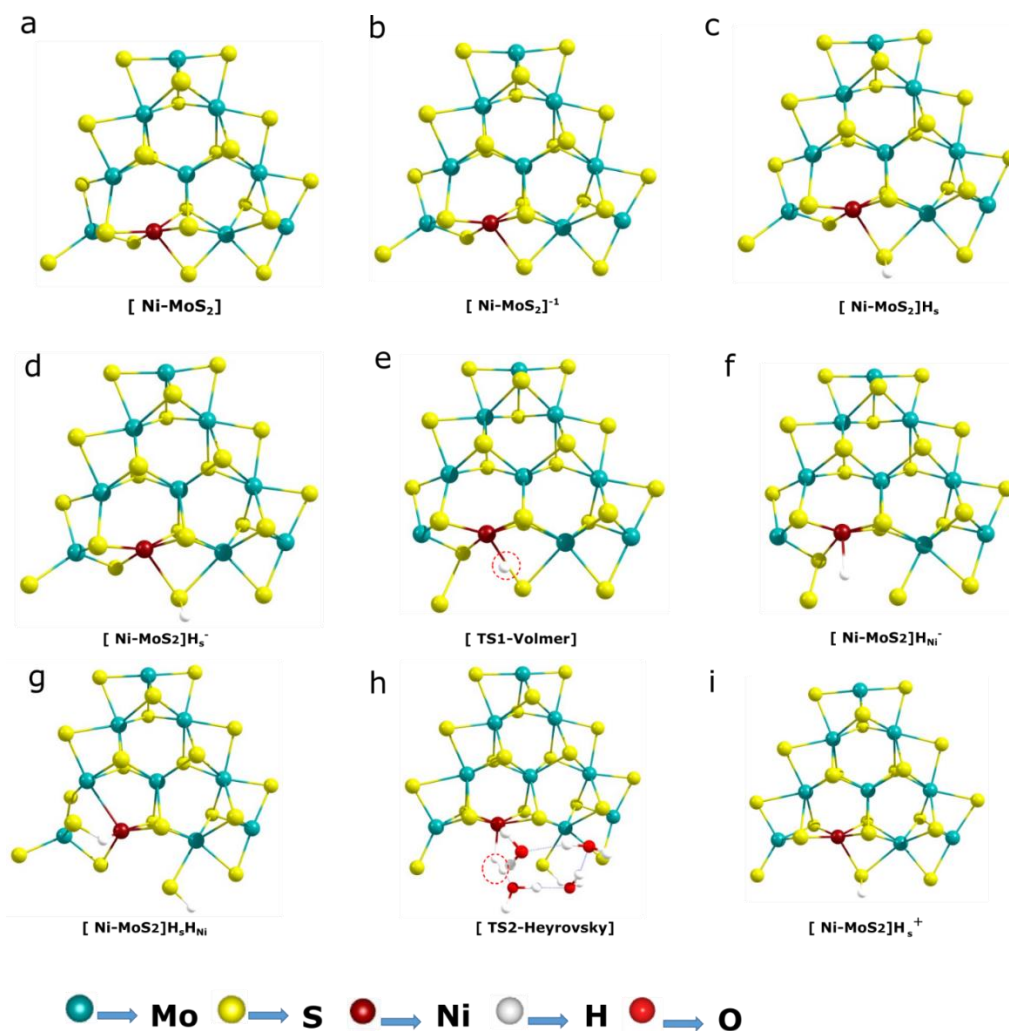


Figure 22: Hydrogen evolution reaction steps for the Ni-MoS₂ materials & optimized geometries of catalysts.

Table 2: Reaction barrier energy of the Ni-MoS₂ materials all the reaction mechanism related materials Performance for HER is shown and there are compared to the experimentally value (solvent phase) materials reported in this Work.

Hydrogen evolution reaction of the Ni-MoS ₂ materials.	Gibbs free energy(ΔG) Kcal/mol (Gas phase)	Energy(Solvent phase) ΔE Kcal/mol
$[\text{Ni-MoS}_2] \rightarrow [\text{Ni-MoS}_2]^{-1}$	-33.06	-44.63
$[\text{Ni-MoS}_2]^{-1} \rightarrow [\text{Ni-MoS}_2] \text{Hs}$	-30.20	-36.06
$[\text{Ni-MoS}_2] \text{Hs} \rightarrow [\text{Ni-MoS}_2]\text{Hs}^-$	-31.49	-44.95
$[\text{Ni-MoS}_2]\text{Hs}^- \rightarrow [\text{Volmer reaction step}]$	Still Running	Still Running
$[\text{Volmer reaction step}] \rightarrow [\text{Ni-MoS}_2] \text{H}_{\text{Ni}}^-$	Still Running	Still Running
$[\text{Ni-MoS}_2]\text{H}_{\text{Ni}}^- \rightarrow [\text{Ni-MoS}_2]\text{HsH}_{\text{Ni}}$	-29.06	-35.8
$[\text{Ni-MoS}_2]\text{HsH}_{\text{Ni}} \rightarrow [\text{Heyrovsky reaction step}]$	21.6	1.478
$[\text{Heyrovsky reaction steps}] \rightarrow [\text{Ni-MoS}_2]\text{Hs}^+$	-26.67	-33.24

Above the Reactions that have a negative ΔG release free energy and are called exergonic reactions. A negative ΔG means that the reactants, or initial state, have more free energy than the products, or final state. Exergonic reactions are also called spontaneous reactions, because they can occur without the addition of energy.

Reactions with a positive ΔG ($\Delta G > 0$), on the other hand, require an input of energy and are called endergonic reactions. Gibbs free energy are positive this energy known as Activation energy. In this case, the products, or final state, have more free energy than the reactants, or initial state. Endergonic reactions are non-spontaneous, meaning that energy must be added before they can proceed.

Conclusions

In summary, we have computationally studied the structural and electronic properties of 2D transition metal dichalcogenides (TMD). The equilibrium structure, geometry, lattice parameters and electronic property calculations of the pristine 2D monolayer 2H phase of the MoS₂ material and Ni-MoS₂ materials was performed by the B3LYP-D3 method. A 2D periodic model was successfully prepared for these two materials to obtain both the band structure and density of states calculations. The present study found that the energy band gap of the pure 2D monolayer MoS₂ materials is about 2.53 eV, and the Ni doped MoS₂ monolayer has zero band gap indicating conductivity in nature. Therefore, we can say that 2D monolayer MoS₂ material behaves like as a semiconductor and a Ni doped MoS₂ material behaves like as conductor, and they may be suitable for a multifaceted electrocatalytic electrode for HER. The 2D single layer Ni-MoS₂ material shows an excellent catalytic performance in HER. The DFT calculations indicate that the high reactivity observed in the Ni-MoS₂ material. We observed a very importance reaction which is H₂ formation in the HER. We got activation energy barrier for H₂ formation is about 21.6 kcal/mol. This lowest activation barrier energy is due to the stabilization of the rate determinant transition state, where the electron density of H₂ formation is favored by the overlap of the d-orbitals and s-orbitals of the H atoms from the transition metals alloys from Ni. The lowest energy barrier for Heyrovsky reaction (H₂ formation) can be found which is in excellent agreement between the theoretical and experimental data. In the conclusion, for H₂ evolution the catalytic activity can be tuned by substituting transition metals forming alloys, thus the “inert” basal planes can be activated.

References

- (1) Liang, K.; Pakhira, S.; Yang, Z.; Nijamudheen, A.; Ju, L.; Wang, M.; Aguirre-Velez, C. I.; Sterbinsky, G. E.; Du, Y.; Feng, Z.; Mendoza-Cortes, J. L.; Yang, Y. S-Doped MoP Nanoporous Layer Toward High-Efficiency Hydrogen Evolution in PH-Universal Electrolyte. *ACS Catalysis* **2019**, *9* (1), 651–659. <https://doi.org/10.1021/acscatal.8b04291>.
- (2) Liang, K.; Marcus, K.; Zhang, S.; Zhou, L.; Li, Y.; De Oliveira, S. T.; Orlovskaya, N.; Sohn, Y. H.; Yang, Y. NiS₂/FeS Holey Film as Freestanding Electrode for High-Performance Lithium Battery. *Advanced Energy Materials* **2017**, *7* (22), 1–6. <https://doi.org/10.1002/aenm.201701309>.
- (3) Liang, K.; Tang, X.; Hu, W. High-Performance Three-Dimensional Nanoporous NiO Film as a Supercapacitor Electrode. *Journal of Materials Chemistry* **2012**, *22* (22), 11062–11067. <https://doi.org/10.1039/c2jm31526b>.
- (4) Yang, Y. A Mini-Review: Emerging All-Solid-State Energy Storage Electrode Materials for Flexible Devices. *Nanoscale* **2020**, *12* (6), 3560–3573. <https://doi.org/10.1039/c9nr08722b>.
- (5) Xie, J.; Xie, Y. Transition Metal Nitrides for Electrocatalytic Energy Conversion: Opportunities and Challenges. *Chemistry - A European Journal* **2016**, *22* (11), 3588–3598. <https://doi.org/10.1002/chem.201501120>.
- (6) Jaramillo, T. F.; Jørgensen, K. P.; Bonde, J.; Nielsen, J. H.; Horch, S.; Chorkendorff, I. Identification of Active Edge Sites for Electrochemical H₂ Evolution from MoS₂ Nanocatalysts. *Science* **2007**, *317* (5834), 100–102. <https://doi.org/10.1126/science.1141483>.
- (7) Pumera, M.; Sofer, Z.; Ambrosi, A. Layered Transition Metal Dichalcogenides for Electrochemical Energy Generation and Storage. *Journal of Materials Chemistry A* **2014**, *2* (24), 8981–8987. <https://doi.org/10.1039/c4ta00652f>.
- (8) Merki, D.; Hu, X. Recent Developments of Molybdenum and Tungsten Sulfides as Hydrogen Evolution Catalysts. *Energy and Environmental Science* **2011**, *4* (10), 3878–3888. <https://doi.org/10.1039/c1ee01970h>.

- (9) Xie, J.; Xie, Y. Structural Engineering of Electrocatalysts for the Hydrogen Evolution Reaction: Order or Disorder? *ChemCatChem* **2015**, *7* (17), 2568–2580. <https://doi.org/10.1002/cctc.201500396>.
- (10) Yan, Y.; Xia, B.; Ge, X.; Liu, Z.; Wang, J. Y.; Wang, X. Ultrathin MoS₂ Nanoplates with Rich Active Sites as Highly Efficient Catalyst for Hydrogen Evolution. *ACS Applied Materials and Interfaces* **2013**, *5* (24), 12794–12798. <https://doi.org/10.1021/am404843b>.
- (11) Pakhira, S.; Lucht, K. P.; Mendoza-Cortes, J. L. Dirac Cone in Two Dimensional Bilayer Graphene by Intercalation with V, Nb, and Ta Transition Metals. *Journal of Chemical Physics* **2018**, *148* (6). <https://doi.org/10.1063/1.5008996>.
- (12) Xie, J.; Qu, H.; Xin, J.; Zhang, X.; Cui, G.; Zhang, X.; Bao, J.; Tang, B.; Xie, Y. Defect-Rich MoS₂ Nanowall Catalyst for Efficient Hydrogen Evolution Reaction. *Nano Research* **2017**, *10* (4), 1178–1188. <https://doi.org/10.1007/s12274-017-1421-x>.
- (13) Huang, H.; Huang, W.; Yang, Z.; Huang, J.; Lin, J.; Liu, W.; Liu, Y. Strongly Coupled MoS₂ Nanoflake-Carbon Nanotube Nanocomposite as an Excellent Electrocatalyst for Hydrogen Evolution Reaction. *Journal of Materials Chemistry A* **2017**, *5* (4), 1558–1566. <https://doi.org/10.1039/c6ta09612c>.
- (14) Ye, T. N.; Lv, L. B.; Xu, M.; Zhang, B.; Wang, K. X.; Su, J.; Li, X. H.; Chen, J. S. Hierarchical Carbon Nanopapers Coupled with Ultrathin MoS₂ Nanosheets: Highly Efficient Large-Area Electrodes for Hydrogen Evolution. *Nano Energy* **2015**, *15*, 335–342. <https://doi.org/10.1016/j.nanoen.2015.04.033>.
- (15) Guo, Y.; Zhang, X.; Zhang, X.; You, T. Defect- and S-Rich Ultrathin MoS₂ Nanosheet Embedded N-Doped Carbon Nanofibers for Efficient Hydrogen Evolution. *Journal of Materials Chemistry A* **2015**, *3* (31), 15927–15934. <https://doi.org/10.1039/c5ta03766b>.
- (16) Tang, C.; Wang, W.; Sun, A.; Qi, C.; Zhang, D.; Wu, Z.; Wang, D. Sulfur-Decorated Molybdenum Carbide Catalysts for Enhanced Hydrogen Evolution. *ACS Catalysis* **2015**, *5* (11), 6956–6963. <https://doi.org/10.1021/acscatal.5b01803>.
- (17) Xie, J.; Zhang, J.; Li, S.; Grote, F.; Zhang, X.; Zhang, H.; Wang, R.; Lei, Y.; Pan, B.; Xie,

- Y. Controllable Disorder Engineering in Oxygen-Incorporated MoS₂ Ultrathin Nanosheets for Efficient Hydrogen Evolution. *Journal of the American Chemical Society* **2013**, *135* (47), 17881–17888. <https://doi.org/10.1021/ja408329q>.
- (18) Xie, J.; Li, S.; Zhang, X.; Zhang, J.; Wang, R.; Zhang, H.; Pan, B.; Xie, Y. Atomically-Thin Molybdenum Nitride Nanosheets with Exposed Active Surface Sites for Efficient Hydrogen Evolution. *Chemical Science* **2014**, *5* (12), 4615–4620. <https://doi.org/10.1039/c4sc02019g>.
- (19) Wang, H.; Tsai, C.; Kong, D.; Chan, K.; Abild-Pedersen, F.; Nørskov, J. K.; Cui, Y. Transition-Metal Doped Edge Sites in Vertically Aligned MoS₂ Catalysts for Enhanced Hydrogen Evolution. *Nano Research* **2015**, *8* (2), 566–575. <https://doi.org/10.1007/s12274-014-0677-7>.
- (20) Merki, D.; Vrubel, H.; Rovelli, L.; Fierro, S.; Hu, X. Fe, Co, and Ni Ions Promote the Catalytic Activity of Amorphous Molybdenum Sulfide Films for Hydrogen Evolution. *Chemical Science* **2012**, *3* (8), 2515–2525. <https://doi.org/10.1039/c2sc20539d>.
- (21) Tedstone, A. A.; Lewis, D. J.; O'Brien, P. Synthesis, Properties, and Applications of Transition Metal-Doped Layered Transition Metal Dichalcogenides. *Chemistry of Materials* **2016**, *28* (7), 1965–1974. <https://doi.org/10.1021/acs.chemmater.6b00430>.
- (22) Lei, Y.; Pakhira, S.; Fujisawa, K.; Wang, X.; Iyiola, O. O.; Perea López, N.; Laura Elías, A.; Pulickal Rajukumar, L.; Zhou, C.; Kabius, B.; Alem, N.; Endo, M.; Lv, R.; Mendoza-Cortes, J. L.; Terrones, M. Low-Temperature Synthesis of Heterostructures of Transition Metal Dichalcogenide Alloys (W_xMo_{1-x}S₂) and Graphene with Superior Catalytic Performance for Hydrogen Evolution. *ACS Nano* **2017**, *11* (5), 5103–5112. <https://doi.org/10.1021/acsnano.7b02060>.
- (23) Niu, W.; Pakhira, S.; Marcus, K.; Li, Z.; Mendoza-Cortes, J. L.; Yang, Y. Apically Dominant Mechanism for Improving Catalytic Activities of N-Doped Carbon Nanotube Arrays in Rechargeable Zinc–Air Battery. *Advanced Energy Materials* **2018**, *8* (20). <https://doi.org/10.1002/aenm.201800480>.
- (24) O'M Bockris, J. The Mechanism of the Hydrogen Evolution Reaction on Platinum, Silver,

- and Tungsten Surfaces in Acid Solutions: Correction [1]. *Journal of Physical Chemistry* **1958**, 62 (6), 766. <https://doi.org/10.1021/j150564a037>.
- (25) Sheng, W.; Gasteiger, H. A.; Shao-Horn, Y. Hydrogen Oxidation and Evolution Reaction Kinetics on Platinum: Acid vs Alkaline Electrolytes. *Journal of The Electrochemical Society* **2010**, 157 (11), B1529. <https://doi.org/10.1149/1.3483106>.
- (26) Kong, D.; Wang, H.; Cha, J. J.; Pasta, M.; Koski, K. J.; Yao, J.; Cui, Y. Synthesis of MoS₂ and MoSe₂ Films with Vertically Aligned Layers. *Nano Letters* **2013**, 13 (3), 1341–1347. <https://doi.org/10.1021/nl400258t>.
- (27) Li, Y.; Wang, H.; Xie, L.; Liang, Y.; Hong, G.; Dai, H. The Hydrogen Evolution Reaction. **2011**, 7296–7299.
- (28) Yang, J.; Shin, H. S. Recent Advances in Layered Transition Metal Dichalcogenides for Hydrogen Evolution Reaction. *Journal of Materials Chemistry A* **2014**, 2 (17), 5979–5985. <https://doi.org/10.1039/c3ta14151a>.
- (29) Tributsch, H.; Bennett, J. C. Electrochemistry and Photochemistry of MoS₂ Layer Crystals. I. *Journal of Electroanalytical Chemistry* **1977**, 81 (1), 97–111. [https://doi.org/10.1016/S0022-0728\(77\)80363-X](https://doi.org/10.1016/S0022-0728(77)80363-X).
- (30) Voiry, D.; Yamaguchi, H.; Li, J.; Silva, R.; Alves, D. C. B.; Fujita, T.; Chen, M.; Asefa, T.; Shenoy, V. B.; Eda, G.; Chhowalla, M. Enhanced Catalytic Activity in Strained Chemically Exfoliated WS₂ Nanosheets for Hydrogen Evolution. *Nature Materials* **2013**, 12 (9), 850–855. <https://doi.org/10.1038/nmat3700>.
- (31) Lukowski, M. A.; Daniel, A. S.; Meng, F.; Forticaux, A.; Li, L.; Jin, S. Enhanced Hydrogen Evolution Catalysis from Chemically Exfoliated Metallic MoS₂ Nanosheets. *Journal of the American Chemical Society* **2013**, 135 (28), 10274–10277. <https://doi.org/10.1021/ja404523s>.
- (32) Roy, K.; Padmanabhan, M.; Goswami, S.; Sai, T. P.; Ramalingam, G.; Raghavan, S.; Ghosh, A. Graphene-MoS₂ Hybrid Structures for Multifunctional Photoresponsive Memory Devices. *Nature Nanotechnology* **2013**, 8 (11), 826–830.

<https://doi.org/10.1038/nnano.2013.206>.

- (33) Balamurugan, J.; Peera, S. G.; Guo, M.; Nguyen, T. T.; Kim, N. H.; Lee, J. H. A Hierarchical 2D Ni-Mo-S Nanosheet@nitrogen Doped Graphene Hybrid as a Pt-Free Cathode for High-Performance Dye Sensitized Solar Cells and Fuel Cells. *Journal of Materials Chemistry A* **2017**, *5* (34), 17896–17908. <https://doi.org/10.1039/c7ta04807f>.
- (34) Gao, M. Y.; Yang, C.; Zhang, Q. B.; Zeng, J. R.; Li, X. T.; Hua, Y. X.; Xu, C. Y.; Dong, P. Facile Electrochemical Preparation of Self-Supported Porous Ni-Mo Alloy Microsphere Films as Efficient Bifunctional Electrocatalysts for Water Splitting. *Journal of Materials Chemistry A* **2017**, *5* (12), 5797–5805. <https://doi.org/10.1039/c6ta10812a>.
- (35) Jiang, N.; Tang, Q.; Sheng, M.; You, B.; Jiang, D. E.; Sun, Y. Nickel Sulfides for Electrocatalytic Hydrogen Evolution under Alkaline Conditions: A Case Study of Crystalline NiS, NiS₂, and Ni₃S₂ Nanoparticles. *Catalysis Science and Technology* **2016**, *6* (4), 1077–1084. <https://doi.org/10.1039/c5cy01111f>.
- (36) Salem, R. R. Theory of the Electrolysis of Water. *Protection of Metals* **2008**, *44* (2), 120–125. <https://doi.org/10.1007/s11124-008-2002-x>.
- (37) Koper, M.; Workshop, E. Electron-Proton Transfer Theory and Electrocatalysis Part I.
- (38) Lin, Y. C.; Lu, N.; Perea-Lopez, N.; Li, J.; Lin, Z.; Peng, X.; Lee, C. H.; Sun, C.; Calderin, L.; Browning, P. N.; Bresnehan, M. S.; Kim, M. J.; Mayer, T. S.; Terrones, M.; Robinson, J. A. Direct Synthesis of van Der Waals Solids. *ACS Nano* **2014**, *8* (4), 3715–3723. <https://doi.org/10.1021/nn5003858>.
- (39) Shi, Y.; Zhou, W.; Lu, A. Y.; Fang, W.; Lee, Y. H.; Hsu, A. L.; Kim, S. M.; Kim, K. K.; Yang, H. Y.; Li, L. J.; Idrobo, J. C.; Kong, J. Van Der Waals Epitaxy of MoS₂ Layers Using Graphene as Growth Templates. *Nano Letters* **2012**, *12* (6), 2784–2791. <https://doi.org/10.1021/nl204562j>.
- (40) Yang, J.; Voiry, D.; Ahn, S. J.; Kang, D.; Kim, A. Y.; Chhowalla, M.; Shin, H. S. Two-Dimensional Hybrid Nanosheets of Tungsten Disulfide and Reduced Graphene Oxide as Catalysts for Enhanced Hydrogen Evolution. *Angewandte Chemie - International Edition*

- 2013**, 52 (51), 13751–13754. <https://doi.org/10.1002/anie.201307475>.
- (41) Altavilla, C.; Sarno, M.; Ciambelli, P. A Novel Wet Chemistry Approach for the Synthesis of Hybrid 2D Free-Floating Single or Multilayer Nanosheets of MS₂@oleylamine (M=Mo, W). *Chemistry of Materials* **2011**, 23 (17), 3879–3885. <https://doi.org/10.1021/cm200837g>.
- (42) Liu, K. K.; Zhang, W.; Lee, Y. H.; Lin, Y. C.; Chang, M. T.; Su, C. Y.; Chang, C. S.; Li, H.; Shi, Y.; Zhang, H.; Lai, C. S.; Li, L. J. Growth of Large-Area and Highly Crystalline MoS₂ Thin Layers on Insulating Substrates. *Nano Letters* **2012**, 12 (3), 1538–1544. <https://doi.org/10.1021/nl2043612>.
- (43) Zhan, Y.; Liu, Z.; Najmaei, S.; Ajayan, P. M.; Lou, J. Large-Area Vapor-Phase Growth and Characterization of MoS₂ Atomic Layers on a SiO₂ Substrate. *Small* **2012**, 8 (7), 966–971. <https://doi.org/10.1002/sml.201102654>.
- (44) Gutiérrez, H. R.; Perea-López, N.; Elías, A. L.; Berkdemir, A.; Wang, B.; Lv, R.; López-Urías, F.; Crespi, V. H.; Terrones, H.; Terrones, M. Extraordinary Room-Temperature Photoluminescence in Triangular WS₂ Monolayers. *Nano Letters* **2013**, 13 (8), 3447–3454. <https://doi.org/10.1021/nl3026357>.
- (45) Gong, Y.; Liu, Z.; Lupini, A. R.; Shi, G.; Lin, J.; Najmaei, S.; Lin, Z.; Elías, A. L.; Berkdemir, A.; You, G.; Terrones, H.; Terrones, M.; Vajtai, R.; Pantelides, S. T.; Pennycook, S. J.; Lou, J.; Zhou, W.; Ajayan, P. M. Band Gap Engineering and Layer-by-Layer Mapping of Selenium-Doped Molybdenum Disulfide. *Nano Letters* **2014**, 14 (2), 442–449. <https://doi.org/10.1021/nl4032296>.
- (46) Randich, E.; Gerlach, T. M. Chemical Vapor Deposition. *Bulletin of Alloy Phase Diagrams* **1982**, 3 (2), 140. <https://doi.org/10.1007/BF02892363>.
- (47) Hui, J.; Schorr, N. B.; Pakhira, S.; Qu, Z.; Mendoza-Cortes, J. L.; Rodríguez-López, J. Achieving Fast and Efficient K⁺ Intercalation on Ultrathin Graphene Electrodes Modified by a Li⁺ Based Solid-Electrolyte Interphase. *Journal of the American Chemical Society* **2018**, 140 (42). <https://doi.org/10.1021/jacs.8b08907>.

- (48) Pakhira, S.; Lucht, K. P.; Mendoza-Cortes, J. L. Dirac Cone in Two Dimensional Bilayer Graphene by Intercalation with V, Nb, and Ta Transition Metals. *arXiv* **2017**, 064707.
- (49) Roy, S.; Sinha, N.; Pakhira, S.; Chakraborty, C. Generation of Emissive Nanosphere from Micro-Aggregates in Anionic Perylene Diimide: Co-Relation of Self-Assembly, Emission, and Electrical Properties. *Dyes and Pigments* **2021**, 192.
<https://doi.org/10.1016/j.dyepig.2021.109461>.
- (50) Puttaswamy, R.; Nagaraj, R.; Kulkarni, P.; Beere, H. K.; Upadhyay, S. N.; Balakrishna, R. G.; Sanna Kotrapannavar, N.; Pakhira, S.; Ghosh, D. Constructing a High-Performance Aqueous Rechargeable Zinc-Ion Battery Cathode with Self-Assembled Mat-like Packing of Intertwined Ag(I) Pre-Inserted V₃O₇·H₂O Microbelts with Reduced Graphene Oxide Core. *ACS Sustainable Chemistry and Engineering* **2021**, 9 (11).
<https://doi.org/10.1021/acssuschemeng.0c06147>.
- (51) Dharmawardana, M.; Pakhira, S.; Welch, R. P.; Caicedo-Narvaez, C.; Luzuriaga, M. A.; Arimilli, B. S.; McCandless, G. T.; Fahimi, B.; Mendoza-Cortes, J. L.; Gassensmith, J. J. Rapidly Reversible Organic Crystalline Switch for Conversion of Heat into Mechanical Energy. *Journal of the American Chemical Society* **2021**.
<https://doi.org/10.1021/jacs.1c01549>.
- (52) Sonkar, C.; Malviya, N.; Sinha, N.; Mukherjee, A.; Pakhira, S.; Mukhopadhyay, S. Selective Anticancer Activities of Ruthenium(II)-Tetrazole Complexes and Their Mechanistic Insights. *BioMetals* **2021**. <https://doi.org/10.1007/s10534-021-00308-x>.
- (53) Sen, K.; Ghosh, D.; Pakhira, S.; Banu, T.; Das, A. K. Structure, Stability, and Dissociation of Small Ionic Silicon Oxide Clusters [SiO_n⁺ (n = 3, 4)]: Insight from Density Functional and Topological Exploration. *Journal of Chemical Physics* **2013**, 139 (23).
<https://doi.org/10.1063/1.4840455>.
- (54) Pakhira, S.; Lucht, K. P.; Mendoza-Cortes, J. L. Iron Intercalation in Covalent-Organic Frameworks: A Promising Approach for Semiconductors. *Journal of Physical Chemistry C* **2017**, 121 (39). <https://doi.org/10.1021/acs.jpcc.7b06617>.
- (55) Hay, P. J.; Wadt, W. R. Ab Initio Effective Core Potentials for Molecular Calculations.

- Potentials for the Transition Metal Atoms Sc to Hg. *The Journal of Chemical Physics* **1985**, 82 (1), 270–283. <https://doi.org/10.1063/1.448799>.
- (56) Cora, F.; Patel, A.; Harrison, N.; Roetti, C.; Catlow, C. An Ab Initio Hartree – Fock Study of a -MoO₃. *Royal Society of Chemistry* **1997**, 7, 959–967.
- (57) Pakhira, S.; Das, A. K. Spectroscopy and Dissociation of I₂-Rg (Rg = Kr and Xe) van Der Waals Complexes. *Theoretical Chemistry Accounts* **2011**, 130 (1). <https://doi.org/10.1007/s00214-011-0978-9>.
- (58) Pakhira, S.; Mondal, B.; Das, A. K. Spectroscopic Properties of I₂-Rg (Rg = He, Ne, Ar) van Der Waals Complexes. *Chemical Physics Letters* **2011**, 505 (4–6). <https://doi.org/10.1016/j.cplett.2011.01.062>.
- (59) Pakhira, S.; Sahu, C.; Sen, K.; Das, A. K. Can Two T-Shaped Isomers of OCS-C₂H₂ van Der Waals Complex Exist? *Chemical Physics Letters* **2012**, 549. <https://doi.org/10.1016/j.cplett.2012.08.043>.
- (60) Pakhira, S.; Dasa, A. K. Spectroscopic Properties, Potential Energy Surfaces and Interaction Energies of RgClF (Rg = Kr and Xe) van Der Waals Complexes. *European Physical Journal D* **2012**, 66 (5). <https://doi.org/10.1140/epjd/e2012-30110-9>.
- (61) Pakhira, S.; Mandal, D.; Mondal, B.; Das, A. K. Theoretical Study of Spectroscopy, Interaction, and Dissociation of Linear and T-Shaped Isomers of RgClF (Rg = He, Ne, and Ar) van Der Waals Complexes. *Structural Chemistry* **2012**, 23 (3). <https://doi.org/10.1007/s11224-011-9914-9>.
- (62) Baker, J.; Scheiner, A.; Andzelm, J. Spin Contamination in Density Functional Theory. *Chemical Physics Letters* **1993**, 216 (3–6), 380–388. [https://doi.org/10.1016/0009-2614\(93\)90113-F](https://doi.org/10.1016/0009-2614(93)90113-F).
- (63) Pakhira, S.; Sahu, C.; Sen, K.; Das, A. K. Dispersion Corrected Double High-Hybrid and Gradient-Corrected Density Functional Theory Study of Light Cation-Dihydrogen (M⁺-H₂, Where M = Li, Na, B and Al) van Der Waals Complexes. *Structural Chemistry* **2013**, 24 (2). <https://doi.org/10.1007/s11224-012-0107-y>.

- (64) Takayanagi, M.; Pakhira, S.; Nagaoka, M. Control of Diffusion and Conformation Behavior of Methyl Methacrylate Monomer by Phenylene Fin in Porous Coordination Polymers. *Journal of Physical Chemistry C* **2015**, *119* (49).
<https://doi.org/10.1021/acs.jpcc.5b09332>.
- (65) Pakhira, S.; Debnath, T.; Sen, K.; Das, A. K. Role of Double-Hybrid Density Functionals and Correlation Consistent Basis Sets in OCS-Hydrocarbon Complexes. *Indian Journal of Chemistry - Section A Inorganic, Physical, Theoretical and Analytical Chemistry* **2015**, *54A* (11), 1369–1377.
- (66) Sinha, N.; Pakhira, S. Tunability of the Electronic Properties of Covalent Organic Frameworks. *ACS Applied Electronic Materials* **2021**, *3* (2).
<https://doi.org/10.1021/acsaelm.0c00867>.
- (67) Dovesi, R.; Erba, A.; Orlando, R.; Zicovich-Wilson, C. M.; Civalleri, B.; Maschio, L.; Rérat, M.; Casassa, S.; Baima, J.; Salustro, S.; Kirtman, B. Quantum-Mechanical Condensed Matter Simulations with CRYSTAL. *Wiley Interdisciplinary Reviews: Computational Molecular Science* **2018**, *8* (4), 1–36. <https://doi.org/10.1002/wcms.1360>.
- (68) Dovesi, R.; Pascale, F.; Civalleri, B.; Doll, K.; Harrison, N. M.; Bush, I.; D'Arco, P.; Noël, Y.; Rérat, M.; Carbonnière, P.; Causà, M.; Salustro, S.; Lacivita, V.; Kirtman, B.; Ferrari, A. M.; Gentile, F. S.; Baima, J.; Ferrero, M.; Demichelis, R.; De La Pierre, M. The CRYSTAL Code, 1976-2020 and beyond, a Long Story. *The Journal of chemical physics* **2020**, *152* (20), 204111. <https://doi.org/10.1063/5.0004892>.
- (69) Allouche, A. Software News and Updates Gabedit — A Graphical User Interface for Computational Chemistry Softwares. *Journal of computational chemistry* **2012**, *32*, 174–182. <https://doi.org/10.1002/jcc>.
- (70) Grimme, S.; Antony, J.; Ehrlich, S.; Krieg, H. A Consistent and Accurate Ab Initio Parametrization of Density Functional Dispersion Correction (DFT-D) for the 94 Elements H-Pu. *Journal of Chemical Physics* **2010**, *132* (15).
<https://doi.org/10.1063/1.3382344>.
- (71) Pakhira, S.; Sen, K.; Sahu, C.; Das, A. K. Performance of Dispersion-Corrected Double

- Hybrid Density Functional Theory: A Computational Study of OCS-Hydrocarbon van Der Waals Complexes. *Journal of Chemical Physics* **2013**, *138* (16).
<https://doi.org/10.1063/1.4802247>.
- (72) Pakhira, S.; Takayanagi, M.; Nagaoka, M. Diverse Rotational Flexibility of Substituted Dicarboxylate Ligands in Functional Porous Coordination Polymers. *Journal of Physical Chemistry C* **2015**, *119* (52), 28789–28799. <https://doi.org/10.1021/acs.jpcc.5b10393>.
- (73) Heyd, J.; Scuseria, G. E.; Ernzerhof, M. Hybrid Functionals Based on a Screened Coulomb Potential. *Journal of Chemical Physics* **2003**, *118* (18), 8207–8215.
<https://doi.org/10.1063/1.1564060>.
- (74) Heyd, J.; Peralta, J. E.; Scuseria, G. E.; Martin, R. L. Energy Band Gaps and Lattice Parameters Evaluated with the Heyd-Scuseria-Ernzerhof Screened Hybrid Functional. *Journal of Chemical Physics* **2005**, *123* (17). <https://doi.org/10.1063/1.2085170>.
- (75) Peintinger, M. F.; Oliveira, D. V.; Bredow, T. Consistent Gaussian Basis Sets of Triple-Zeta Valence with Polarization Quality for Solid-State Calculations. *Journal of Computational Chemistry* **2013**, *34* (6), 451–459. <https://doi.org/10.1002/jcc.23153>.
- (76) Pakhira, S.; Lengeling, B. S.; Olatunji-Ojo, O.; Caffarel, M.; Frenklach, M.; Lester, W. A. A Quantum Monte Carlo Study of the Reactions of CH with Acrolein. *Journal of Physical Chemistry A* **2015**, *119* (18), 4214–4223. <https://doi.org/10.1021/acs.jpca.5b00919>.
- (77) Pakhira, S.; Singh, R. I.; Olatunji-Ojo, O.; Frenklach, M.; Lester, W. A. Quantum Monte Carlo Study of the Reactions of CH with Acrolein: Major and Minor Channels. *Journal of Physical Chemistry A* **2016**, *120* (20), 3602–3612.
<https://doi.org/10.1021/acs.jpca.5b11527>.
- (78) Hu, K.; Wu, M.; Hinokuma, S.; Ohto, T.; Wakisaka, M.; Fujita, J. I.; Ito, Y. Boosting Electrochemical Water Splitting: Via Ternary NiMoCo Hybrid Nanowire Arrays. *Journal of Materials Chemistry A* **2019**, *7* (5), 2156–2164. <https://doi.org/10.1039/c8ta11250a>.
- (79) Momma, K.; Izumi, F. VESTA 3 for Three-Dimensional Visualization of Crystal, Volumetric and Morphology Data. *Journal of Applied Crystallography* **2011**, *44* (6),

1272–1276. <https://doi.org/10.1107/S0021889811038970>.

- (80) Duan, X.; Yang, J.; Gao, H.; Ma, J.; Jiao, L.; Zheng, W. Controllable Hydrothermal Synthesis of Manganese Dioxide Nanostructures: Shape Evolution, Growth Mechanism and Electrochemical Properties. *CrystEngComm* **2012**, *14* (12), 4196–4204. <https://doi.org/10.1039/c2ce06587h>.
- (81) Wang, X.; Zhang, F.; Zhu, X.; Xia, B.; Chen, J.; Qiu, S.; Li, J. Decoration of Multiwalled Carbon Nanotubes with CoO and NiO Nanoparticles and Studies of Their Magnetism Properties. *Journal of Colloid and Interface Science* **2009**, *337* (1), 272–277. <https://doi.org/10.1016/j.jcis.2009.05.006>.
- (82) Sen, K.; Pakhira, S.; Sahu, C.; Das, A. K. Theoretical Study of Efficiency of Metal Cations (Mg⁺, Ca⁺, and Ag⁺) for Effective Hydrogen Storage. *Molecular Physics* **2014**, *112* (2), 182–188. <https://doi.org/10.1080/00268976.2013.805849>.
- (83) Bhojane, P.; Sinha, L.; Devan, R. S.; Shirage, P. M. Mesoporous Layered Hexagonal Platelets of Co₃O₄ Nanoparticles with (111) Facets for Battery Applications: High Performance and Ultra-High Rate Capability. *Nanoscale* **2018**, *10* (4), 1779–1787. <https://doi.org/10.1039/c7nr07879j>.
- (84) Zhang, L.; He, W.; Xiang, X.; Li, Y.; Li, F. Roughening of Windmill-Shaped Spinel Co₃O₄ Microcrystals Grown on a Flexible Metal Substrate by a Facile Surface Treatment to Enhance Their Performance in the Oxidation of Water. *RSC Advances* **2014**, *4* (82), 43357–43365. <https://doi.org/10.1039/c4ra07082h>.
- (85) Weina, X.; Guanlin, L.; Chuanshen, W.; Hu, C.; Wang, X. A Novel β -MnO₂ Micro/Nanorod Arrays Directly Grown on Flexible Carbon Fiber Fabric for High-Performance Enzymeless Glucose Sensing. *Electrochimica Acta* **2017**, *225*, 121–128. <https://doi.org/10.1016/j.electacta.2016.12.130>.
- (86) Zhao, Y.; Truhlar, D. G. A New Local Density Functional for Main-Group Thermochemistry, Transition Metal Bonding, Thermochemical Kinetics, and Noncovalent Interactions. *Journal of Chemical Physics* **2006**, *125* (19). <https://doi.org/10.1063/1.2370993>.

- (87) Zhao, Y.; Truhlar, D. G. The M06 Suite of Density Functionals for Main Group Thermochemistry, Thermochemical Kinetics, Noncovalent Interactions, Excited States, and Transition Elements: Two New Functionals and Systematic Testing of Four M06-Class Functionals and 12 Other Function. *Theoretical Chemistry Accounts* **2008**, *120* (1–3), 215–241. <https://doi.org/10.1007/s00214-007-0310-x>.
- (88) Frisch, M. J.; Pople, J. A.; Binkley, J. S. Self-Consistent Molecular Orbital Methods 25. Supplementary Functions for Gaussian Basis Sets. *The Journal of Chemical Physics* **1984**, *80* (7), 3265–3269. <https://doi.org/10.1063/1.447079>.
- (89) Wadt, W. R.; Hay, P. J. Ab Initio Effective Core Potentials for Molecular Calculations. Potentials for Main Group Elements Na to Bi. *The Journal of Chemical Physics* **1985**, *82* (1), 284–298. <https://doi.org/10.1063/1.448800>.
- (90) Frisch, M. J.; Trucks, G. W.; Schlegel, H. B.; Scuseria, G. E.; Robb, M. A.; Cheeseman, J. R.; Scalmani, G.; Barone, V.; Mennucci, B.; Petersson, G. A.; Nakatsuji, H.; Caricato, M.; Li, X.; Hratchian, H. P.; Izmaylov, A. F.; Bloino, J.; Zheng, G.; Sonnenberg, J. L.; Hada, M.; Ehara, M.; Toyota, K.; Fukuda, R.; Hasegawa, J.; Ishida, M.; Nakajima, T.; Honda, Y.; Kitao, O.; Nakai, H.; Vreven, T.; Montgomery, J. A.; Peralta, J. E.; Ogliaro, F.; Bearpark, M.; Heyd, J. J.; Brothers, E.; Kudin, K. N.; Staroverov, V. N.; Kobayashi, R.; Normand, J.; Raghavachari, K.; Rendell, A.; Burant, J. C.; Iyengar, S. S.; Tomasi, J.; Cossi, M.; Rega, N.; Millam, J. M.; Klene, M.; Knox, J. E.; Cross, J. B.; Bakken, V.; Adamo, C.; Jaramillo, J.; Gomperts, R.; Stratmann, R. E.; Yazyev, O.; Austin, A. J.; Cammi, R.; Pomelli, C.; Ochterski, J. W.; Martin, R. L.; Morokuma, K.; Zakrzewski, V. G.; Voth, G. A.; Salvador, P.; Dannenberg, J. J.; Dapprich, S.; Daniels, A. D.; Farkas; Foresman, J. B.; Ortiz, J. V; Cioslowski, J.; Fox, D. J. Gaussian 09, Revision B.01. *Gaussian 09, Revision B.01, Gaussian, Inc., Wallingford CT* **2009**, 1–20.
- (91) Hui, J.; Pakhira, S.; Bhargava, R.; Barton, Z. J.; Zhou, X.; Chinderle, A. J.; Mendoza-Cortes, J. L.; Rodríguez-López, J. Modulating Electrocatalysis on Graphene Heterostructures: Physically Impermeable Yet Electronically Transparent Electrodes. *ACS Nano* **2018**, *12* (3). <https://doi.org/10.1021/acsnano.8b00702>.
- (92) Sahu, C.; Pakhira, S.; Sen, K.; Das, A. K. A Computational Study of Detoxification of

Lewisite Warfare Agents by British Anti-Lewisite: Catalytic Effects of Water and Ammonia on Reaction Mechanism and Kinetics. *Journal of Physical Chemistry A* **2013**, *117* (16). <https://doi.org/10.1021/jp312254z>.

- (93) Garza, A. J.; Pakhira, S.; Bell, A. T.; Mendoza-Cortes, J. L.; Head-Gordon, M. Reaction Mechanism of the Selective Reduction of CO₂ to CO by a Tetraaza [CoIIN₄H]²⁺ Complex in the Presence of Protons. *Physical Chemistry Chemical Physics* **2018**, *20* (37). <https://doi.org/10.1039/c8cp01963k>.